

Alma Mater Studiorum Università di Bologna  
Archivio istituzionale della ricerca

Abundance–diversity relationship as a unique signature of temporal scaling in the fossil record

This is the final peer-reviewed author's accepted manuscript (postprint) of the following publication:

*Published Version:*

Tomašových, A., Kowalewski, M., Nawrot, R., Scarponi, D., Zuschin, M. (2024). Abundance–diversity relationship as a unique signature of temporal scaling in the fossil record. *ECOLOGY LETTERS*, 27(7), 1-15 [10.1111/ele.14470].

*Availability:*

This version is available at: <https://hdl.handle.net/11585/995285> since: 2024-10-31

*Published:*

DOI: <http://doi.org/10.1111/ele.14470>

*Terms of use:*

Some rights reserved. The terms and conditions for the reuse of this version of the manuscript are specified in the publishing policy. For all terms of use and more information see the publisher's website.

This item was downloaded from IRIS Università di Bologna (<https://cris.unibo.it/>).  
When citing, please refer to the published version.

(Article begins on next page)

1 **Abundance-diversity relationship as a unique signature of temporal scaling in the fossil**  
2 **record**

3

4 Adam Tomašových<sup>1\*</sup>, Michał Kowalewski<sup>2</sup>, Rafał Nawrot<sup>3</sup>, Daniele Scarponi<sup>4</sup>, Martin  
5 Zuschin<sup>3</sup>

6

7 <sup>1</sup>Earth Science Institute, Slovak Academy of Sciences, 84005, Bratislava, Slovakia, ORCID:  
8 0000-0002-0471-9480

9 <sup>2</sup>Florida Museum of Natural History, University of Florida, 1659 Museum Road, Gainesville,  
10 FL, ORCID: [0000-0002-8575-4711](https://orcid.org/0000-0002-8575-4711)

11 <sup>3</sup>Department of Palaeontology, University of Vienna, Josef-Holaubek-Platz 2, 1090 Vienna,  
12 Austria, ORCID: [0000-0002-5774-7311](https://orcid.org/0000-0002-5774-7311), [0000-0002-5235-0198](https://orcid.org/0000-0002-5235-0198)

13 <sup>4</sup>Dipartimento di Scienze Biologiche, Geologiche e Ambientali, University of Bologna, Via  
14 Zamboni 67, 40126 Bologna, Italy, ORCID: [0000-0001-5914-4947](https://orcid.org/0000-0001-5914-4947)

15 \*Corresponding author: Adam Tomašových, [geoltoma@savba.sk](mailto:geoltoma@savba.sk)

16

17 **Keywords:** paleoecology, macroecology, species diversity, species-time relationship,  
18 Holocene, time averaging

19 **Author Contributions:** A.T, M.K., R.N., D.S. and M.Z. designed research, collected data,  
20 and performed analyses; A.T wrote the initial draft, and A.T, M.K., R.N., D.S. and M.Z.  
21 contributed to the final version.

22 **Competing Interest Statement:** The authors declare no competing interest.

23 **Running title:** Temporal scaling of fossil-record diversity

24 Abstract: 149 words

25 Main Text: 5126 words

26 Number of figures: 6

27 Number of references: 81

28 Supporting text

29 Figures S1-S11

30 Tables S1-S5 (separate files)

31 SI references

32 Data files and scripts at Dryad-Zenodo:

33 <https://doi.org/10.5061/dryad.fttdz0903>

34 <https://doi.org/10.5281/zenodo.11664933>

35

36

37 **Abstract**

38 Species diversity increases with the temporal grain of samples according to the species-time  
39 relationship, impacting paleoecological analyses because the temporal grain (time averaging)  
40 of fossil assemblages varies by several orders of magnitude. We predict a positive relation  
41 between total abundance and sample size-independent diversity (ADR) in fossil assemblages  
42 because an increase in time averaging, determined by a decreasing sediment accumulation,  
43 should increase abundance and depress species dominance. We demonstrate that, in contrast  
44 to negative ADR of non-averaged living assemblages, the ADR of Holocene fossil  
45 assemblages is positive, unconditionally or when conditioned on the energy availability  
46 gradient. However, the positive fossil ADR disappears when conditioned on sediment  
47 accumulation, demonstrating that ADR is a signature of diversity scaling induced by variable  
48 time averaging. Conditioning ADR on sediment accumulation can identify and remove the  
49 scaling effect caused by time averaging, providing an avenue for unbiased biodiversity  
50 comparisons across space and time.

51

## 52 INTRODUCTION

53 In recent years, ecologists have become increasingly interested in biodiversity dynamics  
54 across timescales, achieving new insights through the integration of neo- and paleoecological  
55 data (Buma et al. 2019; Benito et al. 2020; Pandolfi et al. 2020; Patrick et al. 2021; Dornelas  
56 et al. 2023; Rillo et al. 2022). However, differences in temporal grain of fossil assemblages  
57 and their consequences for diversity patterns need to be accounted for to avoid invalid  
58 inferences (Powell and Kowalewski 2002; Bush and Bambach 2004; Balseiro and Waisfeld  
59 2014; Carlucci and Westrop 2015; Finnegan et al. 2019). Species diversity increases with the  
60 temporal grain of samples as predicted by eco-evolutionary models and observed in  
61 neoecological and paleoecological time series according to the species-time relationship  
62 (STR, Figure 1, Preston 1960, Rosenzweig 1998). Temporal grain of paleoecological samples  
63 is equal to time averaging that corresponds to the cumulative amount of time during which the  
64 individuals forming a fossil assemblage have lived (Kidwell 2013). Estimates of species  
65 diversity thus depend on the time span over which a given assemblage is observed in  
66 neoecological surveys (Adler and Lauenroth 2003; Fridley et al. 2006; Castillo-Escrivà et al.  
67 2020; O'Sullivan et al. 2021) or over which it is incorporated into the stratigraphic record  
68 (Scarponi and Kowalewski 2007; Tomašových and Kidwell 2010a). As marine and terrestrial  
69 environments are characterized by variability in sediment accumulation rate, in disintegration  
70 rate of organismal (typically skeletal) remains, and in their mixing by burrowers (Aller 1982;  
71 Kidwell 1986), time averaging of fossil assemblages in a single paleoecological time series  
72 can vary by several orders of magnitude, from years or decades to multiple millennia or  
73 longer (Scarponi et al. 2013; Tomašových et al. 2016; Ritter et al. 2023). This large variability  
74 in time averaging magnifies the importance of the scaling effect generated by the STR in  
75 paleoecological, as opposed to neoecological time series, in which the temporal grain of  
76 sampling units can be directly controlled.

77 In contrast to neoecological data, estimation of time averaging is challenging in the  
78 fossil record as the accuracy of geochronological tools is limited. Fluctuations in diversity  
79 observed in the fossil record across series of assemblages, which slide up and down along the  
80 STR continuum according to their time averaging, can be thus difficult to distinguish from  
81 changes driven by eco-evolutionary processes. To address this problem, here we formulate a  
82 simple prediction regarding the effect of the variability in temporal grain on the diversity  
83 observed in the fossil record. This prediction, which ultimately can be used to filter out

84 scaling effects on diversity, postulates that the relation between the total fossil abundance and  
85 diversity estimated with methods that remove its dependency on sample size (ADR; Hurlbert  
86 1971; Chao et al. 2014, 2020) will be pulled towards positive values in fossil assemblages  
87 (Figure 2). This prediction relies on the negative effect of *sediment accumulation rate* on both  
88 (1) the abundance of fossils (total abundance of individuals standardized to sediment mass or  
89 volume) and (2) the time averaging of fossil assemblages themselves, which influences the  
90 shape of the species-abundance distribution (Figure 2A, Tomašových and Kidwell 2010b) and  
91 thus species diversity (Šizling et al. 2009; Alroy 2015; Chase et al. 2018; McGlinn et al.  
92 2021).

93 First, in the absence of variability in sedimentation and disintegration, fossil  
94 abundance is a function of both standing abundance and mortality of living populations that  
95 eventually enter as dead individuals into the sediment (Figure 2A). Fossil abundance  
96 integrates this flux of dead individuals into historical layers over variable durations of time  
97 averaging. A decrease in sediment accumulation rate (i.e., in the input of non-skeletal  
98 sediment) will increase the abundance of individuals in fossil assemblages (Kidwell 1986).  
99 Although fossil abundance is also reduced by disintegration rate (Figure 2A), this prediction  
100 is supported empirically as fossil concentrations are associated with stratigraphic surfaces that  
101 result from reduced accumulation rates (Kidwell 1989; Abbott 1997; Egenhoff and Maletz  
102 2007). Second, although the time averaging of fossil assemblages will decline with skeletal  
103 disintegration and will increase with mixing (Figure 2A), the sediment accumulation rate is a  
104 first-order control of time averaging in most settings (Scarponi et al. 2013; Tomašových et al.  
105 2023). Therefore, species diversity of assemblages, measured with indices that are  
106 independent of sample size or use sample size-based or coverage-based rarefaction, will  
107 increase with declining sediment accumulation rate as species dominance and the slope of the  
108 rank-abundance distribution decline with increasing time averaging (steep gray solid lines  
109 scale to flatter dashed lines, right column in Figure 1). This prediction primarily applies to  
110 taxa with high preservation potential in the fossil record (such as calcareous foraminifers,  
111 ostracods or molluscs).

112 Here, we evaluate whether the abundance-diversity relation in fossil assemblages  
113 ( $ADR_F$ ) in the Holocene record of molluscs in the northern Adriatic Sea is positive,  
114 unconditionally or when conditioned on the energy availability gradient (i.e., water depth),  
115 and thus whether it carries the signature of variable time averaging. The abundance-diversity

116 relation independently documented in living assemblages ( $ADR_L$ ) provides a benchmark for  
117 abundance and diversity not affected by time averaging that can be compared with the  $ADR_F$   
118 observed in the fossil record. Based on 26 age-dated sediment cores, we assess the hypotheses  
119 positing (1) that sediment accumulation covaries negatively with fossil abundance and species  
120 diversity, (2) that fossil abundance and species diversity are positively related, either  
121 unconditionally or when conditioned by the energy availability that shapes the  $ADR_L$  in the  
122 northern Adriatic Sea (Figure 2B-I), and (3) are independent when conditioned on sediment  
123 accumulation (Figure 2J-M). To determine whether our findings apply to other taxa, we assess  
124 the  $ADR_L$  and  $ADR_F$  in marine benthic foraminiferal assemblages from different areas  
125 worldwide using data from the Biodeeptime database (Smith et al. 2023).

126

## 127 **CONCEPTUAL FRAMEWORK: PREDICTIONS FROM SPECIES-TIME**

### 128 **RELATIONSHIP INDEPENDENT OF SAMPLE SIZE**

129 The STR is assessed in terms of how the raw species richness increases as a function of  
130 accumulation of temporally-segregated samples. In this approach, diversity increases not only  
131 as a function of increasing temporal grain (time averaging) but also as a function of increasing  
132 sample size. This effect leads to the positive slope of the STR even when the increase in  
133 diversity is driven purely by sampling. Although the contribution of sampling to the STR  
134 slope can be segregated from the ecological processes that induce temporal turnover in  
135 species composition (White et al. 2004, 2006), the STRs can be assessed on the basis of a  
136 sample-size independent diversity, i.e., the Hill-transformed probability of interspecific  
137 encounter (PIE). In Figure 1, we summarize the scaling of this measure as a function of  
138 increasing time averaging in two distinct dispersal-limited metacommunity models. They  
139 differ in the degree of niche equivalence and density-dependence but nevertheless generate  
140 positive STRs by changing the shape of rank-abundance distributions as a consequence of  
141 increasing time averaging. On the one hand, species have equal demographic rates on a per  
142 capita basis in a neutral model, leading to steady-state diversity and an evolving  
143 metacommunity species pool in drift-speciation equilibrium (following Hubbell 2001). On the  
144 other hand, species differ in density-independent niche breadth (standard deviation of the  
145 Gaussian response equal to 0.1 and 0.5 relative to the gradient length of one) and the strength  
146 of interspecific competitive interactions ( $\alpha_{ij} = 0.5$  or  $0.95$ , relative to intraspecific  $\alpha_{ii}$  of 1) in  
147 non-neutral models with constant metacommunity richness (following Thompson et al. 2020).

148 Figure 1 visualizes the model predictions under these scenarios (source scripts in R Core  
149 Team (2021) in the Supplement). Namely, the increase in diversity is associated with the  
150 decline in species dominance and the flattening of rank-abundance distributions (e.g.,  
151 reducing its slope when fitted by the geometric, power-law or power-bend distributions), with  
152 rank abundance distributions of non-averaged assemblages (1 year) being steeper than those  
153 of assemblages time-averaged to 1,000 years. The  $ADR_F$  is predicted to mimic the species-  
154 time relationships because the total abundance is proportional to the product of standing  
155 abundance and the inverse of lifespan, with abundance along the x-axis stretched or squeezed  
156 depending on the lifespan of organisms.

157         The Hill-transformed diversity based on PIE should remain constant with increasing  
158 time averaging only when local assemblages represent random samples from a static  
159 metacommunity pool (sampling model of Coleman, 1981) or from an evolving  
160 metacommunity pool sampled over time spans that are shorter than the time scale of  
161 metacommunity diversification (e.g., over 1,000 years when the mean time of species  
162 originating in a metacommunity is 10,000 years, black lines in Figure 1A). This scenario is  
163 captured by the neutral model and thus can occur when species extinctions due to ecological  
164 drift are in equilibrium with speciation (Hubbell 2001; McGill et al. 2005). The STR slope  
165 will be positive in all other scenarios, determined by processes such as density dependence,  
166 dispersal limitation, or turnover related to habitat filtering (White et al. 2006; Carey et al.  
167 2007; McGlenn and Palmer 2009; Raia et al. 2011). Once the scale of time averaging  
168 approaches the time scale of metacommunity diversification, even randomly assembled  
169 metacommunities will exhibit a positive  $ADR_F$ . The estimates of diversity independent of  
170 sample size (such as the diversity based on PIE) or standardized to the same sampling  
171 completeness (Alroy 2010, Chao et al. 2020) will thus invariably increase with increasing  
172 time averaging. This scaling effect does not necessarily increase the evenness measures that  
173 have species richness in the denominator as the sensitivity of these indices to time averaging  
174 depends on the ratio of higher-order diversity relative to species richness.

175         The theoretical predictions visualized in Figure 1 and in the path diagrams in Figure 2  
176 provide a framework for interpreting the empirical  $ADR_F$ . The ADR can be measured in the  
177 logarithmic space as a regression coefficient specifying the effect of logged abundance on  
178 logged diversity or as a Pearson correlation coefficient between these variables (empirical  
179 species-time relations tend to be power law-like, White et al. 2006). The effects of increasing



180 time averaging that pulls the  $ADR_F$  towards positive values can be visualized in cartoons  
181 depicting the abundance-diversity space and path diagrams in Figure 2. These cartoons  
182 assume that assemblages are subjected to random time averaging that varies by four orders of  
183 magnitude, that the scaling exponent for the Hill-transformed PIE-based diversity is 0.1, and  
184 that the individual lifespan is one year. The abundance and diversity will be positively related  
185 in fossil assemblages varying in time averaging if abundance is unrelated to diversity in living  
186 assemblages (Figure 2B). However, when standing abundance and diversity exhibit a  
187 nonrandom relationship in living assemblages (Chase and Leibold 2002; Storch et al. 2018),  
188 the resulting  $ADR_F$  is a combination of (1) ecological processes driving the  $ADR_L$  (e.g.,  
189 energy or resource availability affecting both variables at yearly or generational scales) and  
190 (2) STR scaling effects (Figure 2B-D). Conditioning the  $ADR_F$  on the gradient in energy  
191 availability that forces the positive or negative  $ADR_L$  will lead to the positive  $ADR_F$  if the  
192 scaling STR effects contribute to variability in diversity (Figure 2F-H). Therefore, the positive  
193  $ADR_F$ , either unconditional or conditioned on the energy availability gradient, can be a  
194 criterion for detecting variability in diversity induced by variability in time averaging in the  
195 fossil record. However, the effect of temporal scaling can be confirmed by conditioning the  
196  $ADR_F$  on sediment accumulation: if this conditioning leads to the independency between  
197 fossil abundance and diversity, the variability in diversity is likely truly triggered by  
198 variability in time averaging (Figure 2J-L). Finally, conditioning the  $ADR_F$  on sediment  
199 accumulation only can be used to infer the original  $ADR_L$  as determined by ecological  
200 processes unrelated to temporal scaling.

201

## 202 MATERIAL AND METHODS

203 ***Study system – macrofaunal assemblages in the Adriatic Sea.*** The northern Adriatic Sea is  
204 one of the few regions where both living assemblages and age-dated, volume-standardized  
205 fossil assemblages were extensively sampled at the scale of the whole basin. We compiled  
206 information on the total standing abundance and diversity of living molluscan communities  
207 from published surveys performed in the late 20<sup>th</sup> and early 21<sup>st</sup> century at water depths  
208 between intertidal and 70 m (Figure S1). This dataset includes 1,150 living assemblage  
209 samples represented by Van Veen grabs (0.1 m<sup>2</sup>) or sediments from 1 m<sup>2</sup> quadrats collected  
210 by scuba divers (Table S1). Data on 489 molluscan fossil samples were compiled from 26  
211 sediment cores collected in the northern Adriatic Sea and Po coastal plain and documented in

212 our former studies (Table S2). Eleven 1-1.5 m-long piston and gravity cores were collected at  
213 12-44 m water depth (Gallmetzer et al. 2016). These cores were split into 4-5 cm-thick  
214 increments; assemblages from all increments were surveyed. Fifteen cores (> 10 m-long)  
215 from the Po coastal plain were split into 5 and 10-cm increments sampled either at 1-3 m  
216 intervals or more densely in the case of frequent facies shifts. Age data for 26 cores were  
217 compiled from the original reports (at least 6 dated levels per core or at least 2 dated levels  
218 per systems tract, Figures S2-S3) and analyzed with Bayesian age-depth models (Blaauw and  
219 Christen 2011) to compute variability in estimates of sediment accumulation rate (cm/y) (see  
220 Supporting Information, Figure S4-S5).

221

222 ***Living and fossil macrofaunal assemblages.*** In all compiled studies, samples of living and  
223 fossil molluscan assemblages were all sieved with a 1 mm mesh size. The abundance of living  
224 molluscan individuals was standardized to 1 m<sup>2</sup>. The fossil abundance was estimated as the  
225 total number of all identifiable molluscan specimens based on exhaustive counting of all  
226 specimens in each increment, or by extrapolating to the total increment volume from sample  
227 splits, and splits standardized to the number of specimens per 1 dm<sup>3</sup> of sediment. Species  
228 diversity was estimated as the Hill-transformed PIE (Hsieh et al. 2016). The minimum raw  
229 (unstandardized) sample size is 10 individuals and the median sample size is 139 individuals.

230 Water depth was measured for living assemblages during sampling and indirectly  
231 estimated for fossil assemblages based on a compositional gradient in non-metric  
232 multidimensional scaling (NMDS). The first axis of NMDS based on the Chord distances and  
233 the proportional abundances of molluscan species orders the Holocene fossil assemblages  
234 along a bathymetric gradient (Figure S6-S7), as documented in former studies (e.g., Wittmer  
235 et al. 2014). To visualize differences in total abundance and diversity between living and  
236 fossil assemblages, we partition living assemblages (shallower and deeper than 10 m) and  
237 fossil assemblages (two main groups detected by a cluster analysis based on the same  
238 abundance data, Figure S8) into two equivalent, onshore (sandy intertidal and fluvially-  
239 influenced nearshore) and offshore (muddy offshore transition and distal prodelta) segments.

240

241 ***Abundance-diversity relationship in macrofaunal assemblages.*** We estimate regression  
242 coefficients specifying the effect of abundance on diversity using the linear mixed-effect

243 models (all variables normalized to z-scores). The effect of fossil abundance on fossil  
244 diversity ( $ADR_F$ ) will vary not only as a function of time averaging but also as a function of  
245 ecological variables (such as energy or resource availability) that jointly affect standing  
246 abundance and diversity of living assemblages ( $ADR_L$ , Figure 2B-D). We use water depth as  
247 such a variable as it affects the diversity and standing abundance of benthic invertebrates  
248 (Tumbiolo and Downing 1994; Cusson and Bourget 2005). Water depth can also covary with  
249 sediment accumulation and thus can confound the effects of sediment accumulation on fossil  
250 diversity or abundance. The effect of water depth is thus partialled out in the assessment of  
251 the two hypotheses postulating that sediment accumulation reduces diversity and abundance  
252 of fossil assemblages. We then assess the corollaries that correspond to three levels of  
253 conditioning (three rows in Figure 2): (1)  $ADR_F$  is unconditionally positive, (2)  $ADR_F$  is  
254 positive when conditioned on an energy availability gradient; and (3)  $ADR_F$  disappears when  
255 the effect of sediment accumulation on  $ADR_F$  is partialled out. The third level is equal to a  
256 structural equation model that finds that the model that incorporates the effect of abundance  
257 on diversity is not better than the model where the covariance between abundance and  
258 diversity is set to zero.

259         To estimate the effect of abundance on diversity, we use the linear mixed-effect  
260 models that account for heterogeneity among cores (with random intercepts and slopes) and  
261 within-core temporal autocorrelations (with a covariate represented by a stratigraphic depth  
262 and the within-core correlation structure modelled by the autoregressive process of order 1,  
263 using the nlme package, Pinheiro et al. 2023). The variation in sediment accumulation,  
264 abundance, and diversity is markedly smaller within cores than among cores (Figure S9), and  
265 the majority of cores in offshore environments were deposited under slow net sediment  
266 accumulation. Therefore, the fixed effects covary with random effects, violating the  
267 assumption of the mixed-effect models. We thus partitioned the fixed effects into within and  
268 between-core effects of abundance and sediment accumulation on diversity in these models  
269 (van de Pol and Wright 2009). Although this approach increases the number of parameters,  
270 the between-core effect of abundance on diversity can be expected to mirror the scaling effect  
271 when time averaging varies primarily among cores. Finally, we use generalized additive  
272 models to visualize the shape of the dependency of abundance and diversity on water depth  
273 and a two-line test to assess whether this dependency along the whole bathymetric gradient is  
274 U-shaped (Simonsohn 2018). We transformed fossil abundance, diversity, and sediment  
275 accumulation to natural logarithms as the empirically documented STRs tend to be

276 approximately linear in the logarithmic space (White et al. 2006) and such transformation also  
277 reduces the skewness of residuals.

278

279 ***Abundance-diversity relationship in microfaunal living and fossil assemblages.*** To assess  
280 the  $ADR_L$  and  $ADR_F$  in another clade, we compiled from the literature (1) 30 surveys of  
281 abundance and diversity in living benthic foraminifers (Table S3); and (2) 73 surveys of  
282 abundance and diversity in fossil benthic foraminifers in Holocene-Pleistocene cores, using  
283 the Biodeeptime database (Smith et al. 2023). We restricted the data to surveys with at least  
284 10 samples with volume- or mass-standardized counts per geographic region or per time  
285 series (Table S4). We quantified the  $ADR_L$  in 30 regions and the  $ADR_F$  at the scale of (1)  
286 individual cores (73 series) and (2) at the scale of larger regions that consist of at least two  
287 cores (25 series). As the  $ADR_L$  is based on modern spatial surveys whereas the  $ADR_F$  is  
288 assessed on the basis of spatio-temporal stratigraphic record, we use a simple Pearson  
289 correlation to compare the  $ADR_L$  and  $ADR_F$  of microfaunal assemblages (generalized least-  
290 squares accounting for temporal autocorrelation led to similar results). All data are available  
291 at <https://doi.org/10.5061/dryad.fttdz0903> and R language scripts at  
292 <https://doi.org/10.5281/zenodo.11664933>.

293

## 294 **RESULTS**

295 ***Effects of sediment accumulation on macrofaunal abundance and diversity.*** Sediment  
296 accumulation in the northern Adriatic Sea declines from ~10 cm/y in onshore deltaic  
297 environments to only ~0.001 cm/y at offshore locations. As predicted, fossil abundance is  
298 affected negatively by sediment accumulation when water depth (energy availability) is  
299 partialled out in mixed-effect models ( $\beta = -0.18$ ,  $p < 0.0001$ , Figure 3A, Table 1). Similarly,  
300 fossil diversity is negatively affected by sediment accumulation in mixed-effect models ( $\beta = -$   
301  $0.18$ ,  $p < 0.0001$ , Figure 3D). Although molluscan abundance declines with water depth in  
302 living assemblages ( $\beta = -0.47$ ,  $p < 0.0001$ , Figure 3B), fossil abundance is invariant to water  
303 depth ( $\beta = 0.02$ ,  $p = 0.37$ , Figure 3C). The PIE-based diversity increases with water depth in  
304 both living ( $\beta = 0.3$ ,  $p < 0.0001$ , Figure 3E) and fossil assemblages ( $\beta = 0.33$ ,  $p = <0.0001$ ,  
305 Figure 3F).

306

307 **Macrofaunal abundance-diversity relation.** The  $ADR_L$  is negative ( $\beta = -1.17$ ,  $p < 0.0001$ ,  
308  $\beta_{depth} = -0.7$ ,  $p < 0.0001$ , Figure 4A). In contrast, the unconditional  $ADR_F$  is generally positive  
309 ( $\beta = 0.72$ ,  $p = 0.03$ ) but rather complex, U-or V-shaped (two-line test with a breakpoint at  
310 diversity = 1.9 separates a negative segment from a positive segment, with  $p < 0.05$ ). The two  
311 maxima in fossil abundance correspond to (1) almost monospecific assemblages in onshore  
312 environments and (2) diverse assemblages in offshore environments (Figure 4B). The linear  
313 mixed-effect model shows that the between-core effect of abundance on diversity is positive  
314 when conditioned on water depth ( $\beta_{depth} = 0.73$ ,  $p < 0.0001$ , Figure 4C) whereas the within-  
315 core abundance effect on diversity is negative ( $\beta_{depth} = -0.023$ ,  $p = 0.029$ ). This contrast  
316 between among-core and within-core abundance effects on diversity is striking when analyses  
317 are limited to offshore environments ( $\beta_{between} = 0.33$ ,  $p < 0.001$ ,  $\beta_{within} = -0.11$ ,  $p = 0.001$ ,  
318 Figure 4D). The unconditional  $ADR_F$  is thus a composite of two patterns: the fossil diversity  
319 does not systematically change with abundance in onshore environments ( $\beta = 0.61$ ,  $p = 0.66$ ,  
320 light gray points in Figure 5A), whereas it increases with abundance in offshore environments  
321 ( $\beta = 0.99$ ,  $p < 0.0001$ , light gray points in Figure 5B), ascending in parallel with increasing  
322 time averaging (contours in Figure 5B).

323

324 **Macrofaunal abundance-diversity relation conditioned by sediment accumulation.** The  
325 *positive* effect of between-core abundance on diversity in mixed-effect models disappears  
326 when conditioned on sediment accumulation ( $\beta = 0.11$ ,  $p = 0.77$ ,  $\beta_{depth} = 0.15$ ,  $p = 0.4$ ). The  
327 within-core abundance has weak negative effects on diversity ( $\beta = -0.025$ ,  $p = 0.08$ ,  $\beta_{depth} = -$   
328  $0.03$ ,  $p = 0.029$ , Table 1). Given that the effect of abundance on diversity is not positive and  
329 that the AIC of the full model that includes the effect of fossil abundance on fossil diversity  
330 (AIC = -3244.6) is only 1.9 units smaller than the AIC of the model that does not incorporate  
331 this effect (AIC = -3242.7), the positive relation between the abundance and diversity of fossil  
332 assemblages is accounted for by the confounding effect of sediment accumulation (Table 1).

333

334 **Microfaunal abundance-diversity relation.**  $ADR_L$  does not show any preference for positive  
335 values (median  $r = -0.18$ ), with six datasets exhibiting a significantly negative  $ADR_L$  and two  
336 datasets (7%) exhibiting a significantly positive  $ADR_L$  (Figure 6, Table S3). 30% of 73  
337 Holocene-Pleistocene cores exhibit a significantly positive (unconditional)  $ADR_F$  (median  $r$   
338  $= 0.08$ , Figure 6, Table S4). This estimate also incorporates environments with low variability

339 in sediment accumulation where the positive  $ADR_F$  is not expected to develop, and thus the  
340 danger of misattributing the observed diversity fluctuations to ecological processes rather than  
341 to the scaling effects is low. When the analyses are restricted to the cores with high variability  
342 in time averaging and abundance, 12 cores exhibit significantly positive  $ADR_F$ , 11 cores show  
343 insignificant  $ADR_F$ , and one core shows significantly negative  $ADR_F$ , thus increasing the  
344 percentage of significantly positive  $ADR_F$  to 50% (Figure S10). Expanding the spatial scale of  
345 microfossil datasets to those with more than one core reduces the number of all datasets to 16  
346 (median  $r = 0.16$ ), among which 50% show a significantly positive  $ADR_F$  (Figure S11).

347

## 348 **DISCUSSION**

349 *Slow sediment accumulation (high time averaging) enhances fossil abundance and*  
350 *diversity.* Our results are consistent with the two predictions positing that both abundance and  
351 diversity decline with increasing sediment accumulation. Therefore, first, time-averaged fossil  
352 abundance is primarily controlled by the lack of dilution by non-skeletal sediment rather than  
353 by ecological forcing of standing abundance of living assemblages at yearly (or generational)  
354 scales covarying with slow sediment accumulation. This conclusion is supported (1) by the  
355 highest abundance of living molluscan assemblages in the Adriatic Sea occurring in the  
356 onshore environments subjected to high sediment accumulation, (2) by the total abundance of  
357 fossil assemblages exceeding that of living assemblages not affected by time averaging by  
358 two orders of magnitude, and by (3) linear mixed-effect models that indicate that the negative  
359 effects of sediment accumulation on fossil abundance are not confounded by other factors.  
360 Second, the decline in sediment accumulation increases the diversity of fossil assemblages in  
361 accordance with the STR. This effect is primarily observed in offshore environments with  
362 variable sediment accumulation where fossil diversity exceeds the standing living diversity by  
363 a factor of ~2-3.

364

365 *Positive  $ADR_F$  as a signature of temporal scaling.* As sediment accumulation reduces both  
366 abundance and diversity, and the positive  $ADR_F$  disappears when conditioned on sediment  
367 accumulation, the variability in abundance and diversity of fossil assemblages is uniquely  
368 driven by variability in time averaging. The negative  $ADR_L$  also indicates that the  $ADR_F$  that  
369 is unconditionally positive or positive when conditioned on the energy availability is simply a

370 consequence of variable sediment accumulation that plays a major role in modulating the  
371 abundance and diversity of fossil assemblages. The effects of STR on the diversity patterns  
372 resulting from variable time averaging of paleontological samples are significant, especially  
373 in offshore environments (i.e., deeper than 10 m), and thus cannot be neglected in diversity  
374 analyses. When cores systematically differ in sediment accumulation (and thus in time  
375 averaging) but within-core variability in sediment accumulation remains relatively low as in  
376 this study, the mixed-effect models effectively separate the scaling effects of time averaging  
377 on the among-site diversity patterns from the ecological effects of abundance on diversity  
378 unrelated to temporal scaling.

379

380 ***Regional  $ADR_F$  shaped by onshore-offshore gradients in time averaging.*** When standing  
381 abundances and diversities of communities are negatively related as in our molluscan dataset  
382 and time averaging differs between onshore and offshore environments (Figure 5A-B),  
383 regional-scale  $ADR_F$  patterns can be complex. In two scenarios in Figure 5C, the initial,  
384 regional-scale  $ADR_L$  is negative in non-averaged assemblages, as observed along the  
385 bathymetric gradient in the Adriatic Sea. In the first scenario, assemblages in four  
386 environments are equally time-averaged and thus the regional-scale  $ADR_F$  can remain  
387 negative due to the absence of variability in temporal scaling (i.e., dashed light-gray arrows in  
388 in Figure 5C). Such  $ADR_F$  can be diagnostic of conditions when the weakly time-averaged  
389 fossil record deposited in eutrophic or oxygen-deficient environments exhibit individual-rich  
390 but species-poor fossil assemblages dominated by opportunistic species (Filipsson and  
391 Nordberg 2004; Tsujimoto et al. 2008). In the second scenario, fossil assemblages in offshore  
392 environments, initially with the smallest abundance, are time-averaged to 2000 years, whereas  
393 assemblages in onshore environments are time-averaged to two years only, leading to the  
394 positive  $ADR_F$  (a dashed dark-gray arrow in Figure 5C). The negative  $ADR_L$  can thus be  
395 reverted into the positive  $ADR_F$  when the most productive assemblages are the least time-  
396 averaged, as observed in our Adriatic data. This indicates that the positive  $ADR_F$  is also  
397 determined by the tendency of individual-rich but species-poor assemblages dominated by  
398 opportunistic species to occur in environments least prone to time averaging. Despite this  
399 additional complexity, the positive  $ADR_F$  is still diagnostic of diversity variability controlled  
400 by the temporal scaling effect.

401

402 *Using ADR to extract ecological signals from fossil assemblages.* Even in the absence of  
403 variability in time averaging, abundance and diversity can be positively associated if they  
404 share a common ecological cause such as the total energy availability, leading to both diverse  
405 and individual-rich assemblages (Hurlbert 2004; Pautasso et al. 2011; Edgar et al. 2017;  
406 Thompson et al. 2020). Therefore, the positive  $ADR_L$  can lead to a false positive result with  
407 respect to the role of time averaging in modulating diversity. However, several lines of  
408 evidence indicate that local-scale  $ADR_L$  is typically not positive. First, our analyses of  
409 molluscan and foraminiferal assemblages and previous studies (Bolam et al. 2002; Covich et  
410 al. 2004; Reiss et al. 2010; Leduc et al. 2012; Schonberg et al. 2014; van der Plas 2019; Dee  
411 et al. 2023; Maureaud et al. 2019; Clare et al. 2022) show that the  $ADR_L$  at local scales is  
412 either negative or close to zero (Figure 6). Second, the  $ADR_F$  of molluscan assemblages  
413 conditioned on sediment accumulation is not positive. Although both total abundance and  
414 biomass are constrained by energy availability that can affect species diversity at local scales,  
415 they are also linked by tradeoffs that can lead to a complex ADR (Kadmon and Benjamini  
416 2006, Dornelas 2010). For example, marine benthic communities dominated by small-sized  
417 species with high abundance tend to be less diverse than communities dominated by larger but  
418 less numerous species (Warwick 1986; Warwick and Clarke 1994). Moreover, species  
419 diversity at local scales is not a simple function of local energy availability because species  
420 extinction is modulated by population sizes at regional scales of species geographic ranges  
421 (attaining few 100s of km or more in marine benthic species). The relationships between  
422 diversity and total number of individuals thus tend to be positive only in studies with regional  
423 and biogeographic sampling grains (Chase and Ryberg 2004; Storch and Okie 2019; Storch et  
424 al. 2018 Craven et al. 2020). The total abundance at local scales is swamped by source-sink  
425 factors and tradeoffs between abundances and biomass and thus local  $ADR_L$  does not simply  
426 scale down from biogeographic  $ADR_L$ . The  $ADR_F$  that is positive unconditionally or when  
427 conditioned on energy availability is thus a useful tool for the detection of scenarios where  
428 variability in diversity at local scales is determined by variability in time averaging. Our  
429 analyses of macro- and microfossil records suggest that this scaling effect is a common,  
430 taxon-independent feature of the fossil record (Fig. 5, Table S4) and thus needs to be  
431 considered when assessing paleoecological data.

432         The effects of temporal scaling can be expected to contribute to fluctuations in local  
433 diversity at longer, million-year time scales not only owing to long-term changes in sediment  
434 accumulation but also owing to secular changes in mixing and disintegration (Kidwell and



435 Brenchley 1994). Time averaging documented in the Cenozoic marine fossil record can attain  
436 more than 100 kyr (Zimmt et al. 2022), further magnifying the scaling effects because time  
437 averaging attaining the scales of species diversification will accelerate species richness  
438 accumulation in the logarithmic STR space (Rosenzweig 1998). Although pooling  
439 assemblages with variable time averaging into million-year (macroevolutionary) bins with  
440 approximately equivalent temporal grain size can alleviate the scaling STR effect, the cost of  
441 such a procedure is the loss of spatial and temporal resolution. The stratigraphic records of  
442 fossil assemblages with well-resolved age models can use sediment accumulation as a  
443 conditioning variable that (1) can remove the biasing effects of differential diversity scaling  
444 caused by variable time averaging and (2) can be used in the mixed-effect models to separate  
445 the scaling STR effect from the original  $ADR_L$  driven by ecological covariance between total  
446 abundance and diversity unrelated to scaling. Conditioning ADR on sediment accumulation  
447 can thus both identify and correct for the scaling effect induced by time averaging when  
448 comparing fossil biodiversity across space and time.

449

#### 450 **Acknowledgements**

451 We thank three reviewers for detailed and critical comments. This research was supported by  
452 the Slovak Research and Development Agency (APVV17-0555, APVV22-0523), Slovak  
453 Scientific Grant Agency (VEGA 02/0106/23), and by the Austrian Science Fund (FWF)  
454 (grant number P24901).

455

#### 456 **References**

457 Aller, R.C., 1982. Carbonate dissolution in nearshore terrigenous muds: the role of physical  
458 and biological reworking. *Journal of Geology*, 90, 79-95.

459 Alroy, J. 2010. The shifting balance of diversity among major marine animal  
460 groups. *Science*, 329, 1191–1194.

461 Alroy, J., 2015. The shape of terrestrial abundance distributions. *Science Advances*, 1,  
462 e1500082.

463 Bell, A., and Kelvyn J. 2015. Explaining Fixed Effects: Random Effects Modeling of Time-  
464 Series Cross-Sectional and Panel Data. *Political Science Research and Methods* 3: 133–53.

465 Abbott, S.T., 1997. Mid-cycle condensed shellbeds from mid-Pleistocene cyclothem, New  
466 Zealand: implications for sequence architecture. *Sedimentology*, 44, 805-824.

467 Adler, P.B. and Lauenroth, W.K., 2003. The power of time: spatiotemporal scaling of species  
468 diversity. *Ecology Letters*, 6, 749-756.

469 Buma, B., Harvey, B.J., Gavin, D.G., Kelly, R., Loboda, T., McNeil, B.E., Marlon, J.R.,  
470 Meddens, A.J.H., Morris, J.L., Raffa, K.F. and Shuman, B., 2019. The value of linking  
471 paleoecological and neoecological perspectives to understand spatially-explicit ecosystem  
472 resilience. *Landscape Ecology*, 34, 17-33.

473 Balseiro, D. and Waisfeld, B.G., 2014. Evenness and diversity in Upper Cambrian–Lower  
474 Ordovician trilobite communities from the Central Andean Basin (Cordillera Oriental,  
475 Argentina). *Palaeontology*, 57, 531-546.

476 Benito, B.M., Gil-Romera, G. and Birks, H.J.B., 2020. Ecological memory at millennial time-  
477 scales: the importance of data constraints, species longevity and niche features. *Ecography*,  
478 43, 1-10.

479 Blaauw, M. and Christen, J.A., 2011. Flexible paleoclimate age-depth models using an  
480 autoregressive gamma process. *Bayesian Analysis* 6:457-474.

481 Bolam, S.G., Fernandes, T.F. and Huxham, M., 2002. Diversity, biomass, and ecosystem  
482 processes in the marine benthos. *Ecological Monographs*, 72, 599-615.

483 Bush, A.M. and Bambach, R.K., 2004. Did alpha diversity increase during the Phanerozoic?  
484 Lifting the veils of taphonomic, latitudinal, and environmental biases. *Journal of*  
485 *Geology*, 112, 625-642.

486 Carey, S., Ostling, A., Harte, J. and del Moral, R., 2007. Impact of curve construction and  
487 community dynamics on the species–time relationship. *Ecology*, 88, 2145-2153.

488 46.

489 Carlucci, J.R. and Westrop, S.R., 2015. Trilobite biofacies and sequence stratigraphy: an  
490 example from the Upper Ordovician of Oklahoma. *Lethaia*, 48, 309-325.

491 Castillo-Escrivà, A., Mesquita-Joanes, F. and Rueda, J., 2020. Effects of the temporal scale of  
492 observation on the analysis of aquatic invertebrate metacommunities. *Frontiers in Ecology*  
493 *and Evolution*, 8, 561838.

494 Chao, A., Gotelli, N.J., Hsieh, T.C., Sander, E.L., Ma, K.H., Colwell, R.K. and Ellison, A.M.,  
495 2014. Rarefaction and extrapolation with Hill numbers: a framework for sampling and  
496 estimation in species diversity studies. *Ecological Monographs*, *84*, 45-67.

497 Chao, A., Kubota, Y., Zelený, D., Chiu, C.H., Li, C.F., Kusumoto, B., Yasuhara, M., Thorn,  
498 S., Wei, C.L., Costello, M.J. and Colwell, R.K., 2020. Quantifying sample completeness and  
499 comparing diversities among assemblages. *Ecological Research*, *35*, 292-314.

500 Chase, J.M. and Leibold, M.A., 2002. Spatial scale dictates the productivity–biodiversity  
501 relationship. *Nature*, *416*, 427-430.

502 Chase, J.M. and Ryberg, W.A., 2004. Connectivity, scale-dependence, and the productivity–  
503 diversity relationship. *Ecology Letters*, *7*, 676-683.

504 Chase, J.M., McGill, B.J., McGlenn, D.J., May, F., Blowes, S.A., Xiao, X., Knight, T.M.,  
505 Purschke, O. and Gotelli, N.J., 2018. Embracing scale-dependence to achieve a deeper  
506 understanding of biodiversity and its change across communities. *Ecology Letters*, *21*, 1737-  
507 1751.

508 Chase, J.M., McGill, B.J., Thompson, P.L., Antão, L.H., Bates, A.E., Blowes, S.A., Dornelas,  
509 M., Gonzalez, A., Magurran, A.E., Supp, S.R. and Winter, M., 2019. Species richness change  
510 across spatial scales. *Oikos*, *128*, 1079-1091.

511 Clare, D.S., Culhane, F. and Robinson, L.A., 2022. Secondary production increases with  
512 species richness but decreases with species evenness of benthic invertebrates. *Oikos*, e08629.

513 Coleman, B.D. 1981. On random placement and species-area relations. *Mathematical*  
514 *Biosciences*, *54*, 191-215.

515 Covich, A.P., Austen, M.C., Bärlocher, F., Chauvet, E., Cardinale, B.J., Biles, C.L., Inchausti,  
516 P., Dangles, O., Solan, M., Gessner, M.O. and Stutzner, B., 2004. The role of biodiversity in  
517 the functioning of freshwater and marine benthic ecosystems. *BioScience*, *54*, 767-775.

518 Craven, D., van der Sande, M.T., Meyer, C., Gerstner, K., Bennett, J.M., Giling, D.P., Hines,  
519 J., Phillips, H.R., May, F., Bannar-Martin, K.H. and Chase, J.M., 2020. A cross-scale  
520 assessment of productivity–diversity relationships. *Global Ecology and Biogeography*, *29*,  
521 1940-1955.

522 Cusson, M. and Bourget, E., 2005. Global patterns of macroinvertebrate production in marine  
523 benthic habitats. *Marine Ecology Progress Series*, 297, 1-14.

524 Dee, L.E., Ferraro, P.J., Severen, C.N., Kimmel, K.A., Borer, E.T., Byrnes, J.E., Clark, A.T.,  
525 Hautier, Y., Hector, A., Raynaud, X. and Reich, P.B., Wright A.J., Arnillas C.A., Davies K.F.,  
526 MacDougall A., Mori A.S., Smith M.D., Adler P.B., Bakker J.D., Brauman K.A., Cowles J.,  
527 Komatsu K., Knops J.M.H., McCulley R.L, Moore J.L., Morgan J.W., Ohlert T., Power S.A.,  
528 Sullivan L.L., Stevens C., and Loreau M. 2023. Clarifying the effect of biodiversity on  
529 productivity in natural ecosystems with longitudinal data and methods for causal  
530 inference. *Nature Communications*, 14, 2607.

531 Dornelas, M., 2010. Disturbance and change in biodiversity. *Philosophical Transactions of*  
532 *the Royal Society*, B365, 3719-3727.

533 Dornelas, M., Chase, J.M., Gotelli, N.J., Magurran, A.E., McGill, B.J., Antão, L.H., Blowes,  
534 S.A., Daskalova, G.N., Leung, B., Martins, I.S. and Moyes, F., 2023. Looking back on  
535 biodiversity change: lessons for the road ahead. *Philosophical Transactions of the Royal*  
536 *Society B*, 378, 20220199.

537 Edgar, G.J., Alexander, T.J., Lefcheck, J.S., Bates, A.E., Kininmonth, S.J., Thomson, R.J.,  
538 Duffy, J.E., Costello, M.J. and Stuart-Smith, R.D., 2017. Abundance and local-scale processes  
539 contribute to multi-phyta gradients in global marine diversity. *Science Advances*, 3, e1700419.

540 Egenhoff, S., and Maletz, J. 2007. Graptolites as indicators of maximum flooding surfaces in  
541 monotonous deep-water shelf successions. *Palaios*, 22, 373–383.

542 Filipsson, H.L. and Nordberg, K., 2004. A 200-year environmental record of a low-oxygen  
543 fjord, Sweden, elucidated by benthic foraminifera, sediment characteristics and hydrographic  
544 data. *Journal of Foraminiferal Research*, 34, 277-293.

545 Finnegan, S., Gehling, J.G. and Droser, M.L., 2019. Unusually variable paleocommunity  
546 composition in the oldest metazoan fossil assemblages. *Paleobiology*, 45, 235-245.

547 Fridley, J.D., Peet, R.K., Van der Maarel, E. and Willems, J.H., 2006. Integration of local and  
548 regional species-area relationships from space-time species accumulation. *American*  
549 *Naturalist*, 168, 133-143.

550 Frignani, M. and Langone, L., 1991. Accumulation rates and <sup>137</sup>Cs distribution in sediments  
551 off the Po River delta and the Emilia-Romagna coast (northwestern Adriatic Sea, Italy).  
552 *Continental Shelf Research*, 11, 525-542.

553 Gallmetzer I., Haselmair A., Stachowitsch M. And Zuschin M. 2016. An innovative piston  
554 corer for large-volume sediment samples. *Limnology and Oceanography: Methods* 14:698–  
555 717.

556 Hsieh, T.C., Ma, K.H. and Chao, A., 2016. iNEXT: an R package for rarefaction and  
557 extrapolation of species diversity (Hill numbers). *Methods in Ecology and Evolution*, 7,  
558 1451-1456.

559 Hubbell, S.P., 2001. The unified neutral theory of biodiversity and biogeography. In *The*  
560 *Unified Neutral Theory of Biodiversity and Biogeography*. Princeton University Press.

561 Hurlbert, S.H., 1971. The Nonconcept of Species Diversity: A Critique and Alternative  
562 Parameters. *Ecology* 52:577-586.

563 Hurlbert, A.H., 2004. Species–energy relationships and habitat complexity in bird  
564 communities. *Ecology Letters*, 7, 714-720.

565 Kadmon, R. and Benjamini, Y., 2006. Effects of productivity and disturbance on species  
566 richness: a neutral model. *American Naturalist*, 167, 939-946.

567 Kidwell, S.M., 1986. Models for fossil concentrations: paleobiologic  
568 implications. *Paleobiology* 12, 6-24.

569 Kidwell, S.M., 1989. Stratigraphic condensation of marine transgressive records: origin of  
570 major shell deposits in the Miocene of Maryland. *Journal of Geology*, 97, 1-24.

571 Kidwell, S.M. and Brenchley, P.J., 1994. Patterns in bioclastic accumulation through the  
572 Phanerozoic: changes in input or in destruction? *Geology*, 22, 1139-1143.

573 Kidwell, S.M., Best, M.M. and Kaufman, D.S., 2005. Taphonomic trade-offs in tropical  
574 marine death assemblages: differential time averaging, shell loss, and probable bias in  
575 siliciclastic vs. carbonate facies. *Geology*, 33, 729-732.

576 Kidwell, S.M., 2013. Time-averaging and fidelity of modern death assemblages: building a  
577 taphonomic foundation for conservation palaeobiology. *Palaeontology*, 56, 487-522.

578 Labra, F.A., Hernández-Miranda, E. and Quinones, R.A., 2015. Dynamic relationships  
579 between body size, species richness, abundance, and energy use in a shallow marine  
580 epibenthic faunal community. *Ecology and Evolution*, 5, 391-408.

581 Leduc, D., Rowden, A.A., Bowden, D.A., Probert, P.K., Pilditch, C.A. and Nodder, S.D.,  
582 2012. Unimodal relationship between biomass and species richness of deep-sea nematodes:  
583 implications for the link between productivity and diversity. *Marine Ecology Progress*  
584 *Series*, 454, 53-64.

585 Maureaud, A., Hodapp, D., Van Denderen, P.D., Hillebrand, H., Gislason, H., Spaanheden  
586 Dencker, T., Beukhof, E. and Lindegren, M., 2019. Biodiversity–ecosystem functioning  
587 relationships in fish communities: biomass is related to evenness and the environment, not to  
588 species richness. *Proceedings of the Royal Society B*, 286, 20191189.

589 McGill, B.J., Hadly, E.A. and Maurer, B.A., 2005. Community inertia of Quaternary small  
590 mammal assemblages in North America. *Proceedings of the National Academy of Sciences*,  
591 102, 16701-16706.

592 McGlinn, D.J. and Palmer, M.W., 2009. Modeling the sampling effect in the species–time–  
593 area relationship. *Ecology*, 90, 836-846.

594 McGlinn, D.J., Engel, T., Blowes, S.A., Gotelli, N.J., Knight, T.M., McGill, B.J., Sanders,  
595 N.J. and Chase, J.M., 2021. A multiscale framework for disentangling the roles of evenness,  
596 density, and aggregation on diversity gradients. *Ecology*, 102, e03233.

597 O’Sullivan, J.D., Terry, J.C.D. and Rossberg, A.G., 2021. Intrinsic ecological dynamics drive  
598 biodiversity turnover in model metacommunities. *Nature Communications*, 12, 3627.

599 Pandolfi, J.M., Staples, T.L. and Kiessling, W., 2020. Increased extinction in the emergence  
600 of novel ecological communities. *Science*, 370, 220-222.

601 Patrick, C.J., McCluney, K.E., Ruhi, A., Gregory, A., Sabo, J. and Thorp, J.H. 2021. Multi-  
602 scale biodiversity drives temporal variability in macrosystems. *Frontiers in Ecology and the*  
603 *Environment*, 19, 47-56.

604 Pautasso, M., Böhning-Gaese, K., Clergeau, P., Cueto, V.R., Dinetti, M., Fernández-Juricic,  
605 E., Kaisanlahti-Jokimäki, M.L., Jokimäki, J., McKinney, M.L., Sodhi, N.S. and Storch, D.,  
606 2011. Global macroecology of bird assemblages in urbanized and semi-natural  
607 ecosystems. *Global Ecology and Biogeography*, 20, 426-436.

608 Pinheiro J, Bates D, R Core Team (2023). nlme: Linear and Nonlinear Mixed Effects Models.  
609 R package version 3.1-164, <https://CRAN.R-project.org/package=nlme>.

610 Powell, M.G. and Kowalewski, M. 2002. Increase in evenness and sampled alpha diversity  
611 through the Phanerozoic: comparison of early Paleozoic and Cenozoic marine fossil  
612 assemblages. *Geology*, 30, 331-334.

613 Preston, F.W., 1960. Time and space and the variation of species. *Ecology*, 41, 612-627.

614 Reiss, H., Degraer, S., Duineveld, G.C., Kröncke, I., Aldridge, J., Craeymeersch, J.A.,  
615 Eggleton, J.D., Hillewaert, H., Lavaleye, M.S., Moll, A. and Pohlmann, T., 2010. Spatial  
616 patterns of infauna, epifauna, and demersal fish communities in the North Sea. *ICES Journal*  
617 *of Marine Science*, 67, 278-293.

618 R Core Team (2021). R: A language and environment for statistical computing. R Foundation  
619 for Statistical Computing, Vienna, Austria. URL <https://www.R-project.org/>.

620 Raia, P., Carotenuto, F., Meloro, C., Piras, P. and Barbera, C. 2011. Species accumulation  
621 over space and time in European Plio-Holocene mammals. *Evolutionary Ecology*, 25, 171-  
622 188.

623 Rillo, M.C., Woolley, S. and Hillebrand, H., 2022. Drivers of global pre-industrial patterns of  
624 species turnover in planktonic foraminifera. *Ecography*, 2022, e05892.

625 Ritter D.N.M., M., Erthal, F., Kosnik, M.A., Kowalewski, M., Coimbra, J.C., Caron, F. and  
626 Kaufman, D.S., 2023. Onshore-offshore trends in the temporal resolution of molluscan death  
627 assemblages: how age-frequency distributions reveal quaternary sea-level  
628 history. *Palaios*, 38, 148-157.

629 Rosenzweig, M.L., 1998. Preston's ergodic conjecture: The accumulation of species in space  
630 and time. In *Biodiversity dynamics*, 311-348. Columbia University Press.

631 Scarponi, D. and Kowalewski M. 2007. Sequence stratigraphic anatomy of diversity patterns:  
632 Late Quaternary benthic mollusks of the Po Plain, Italy. *Palaios*, 22, 296-305.

633 Scarponi, D., Kaufman, D., Amorosi, A. and Kowalewski, M., 2013. Sequence stratigraphy  
634 and the resolution of the fossil record. *Geology*, 41, 239-242.

635 Scheiner, S.M., Chiarucci, A., Fox, G.A., Helmus, M.R., McGlinn, D.J. and Willig, M.R.,  
636 2011. The underpinnings of the relationship of species richness with space and  
637 time. *Ecological Monographs*, 81, 195-213.

638 Schonberg, S.V., Clarke, J.T. and Dunton, K.H., 2014. Distribution, abundance, biomass and  
639 diversity of benthic infauna in the Northeast Chukchi Sea, Alaska: Relation to environmental  
640 variables and marine mammals. *Deep Sea Research Part II: Topical Studies in*  
641 *Oceanography*, 102, 144-163. Simonsohn, U., 2018. Two lines: A valid alternative to the  
642 invalid testing of U-shaped relationships with quadratic regressions. *Advances in Methods and*  
643 *Practices in Psychological Science*, 1, 538-555.

644 Smith J., Rillo M.C., Kocsis Á.T., Dornelas M., Fastovich D., Huang H.H.M., Jonkers L.,  
645 Kiessling W., Li Q., Liow L.H., Margulis-Ohnuma M., Meyers S., Na L., Penny A.,  
646 Pippenger K., Renaudie J., Saupe E.E., Steinbauer M.J., Sugawara M., Tomašových A.,  
647 Williams J.J., Yasuhara M., Finnegan S. and Hull P.M. 2023. BioDeepTime: A database of  
648 biodiversity time series for modern and fossil assemblages. *Global Ecology and*  
649 *Biogeography*, 32, 1680-1689.

650 Storch, D., Bohdalková, E. and Okie, J., 2018. The more-individuals hypothesis revisited: the  
651 role of community abundance in species richness regulation and the productivity–diversity  
652 relationship. *Ecology Letters*, 21, 920-937.

653 Storch, D. and Okie, J.G., 2019. The carrying capacity for species richness. *Global Ecology*  
654 *and Biogeography*, 28, 1519-1532.

655 Šizling, A.L., Storch, D., Šizlingová, E., Reif, J. and Gaston, K.J., 2009. Species abundance  
656 distribution results from a spatial analogy of central limit theorem. *Proceedings of the*  
657 *National Academy of Sciences*, 106, 6691-6695.

658 Thompson, P.L., Guzman, L.M., De Meester, L., Horváth, Z., Ptacnik, R., Vanschoenwinkel,  
659 B., Viana, D.S. and Chase, J.M., 2020. A process-based metacommunity framework linking  
660 local and regional scale community ecology. *Ecology Letters* 23, 1314-1329.

661 Tomašových, A. and Kidwell, S.M., 2010a. The effects of temporal resolution on species  
662 turnover and on testing metacommunity models. *American Naturalist*, 175, 587-606.



663 Tomašových, A. and Kidwell, S.M., 2010b. Predicting the effects of increasing temporal scale  
664 on species composition, diversity, and rank-abundance distributions. *Paleobiology*, 36, 672-  
665 695.

666 Tomašových, A., Kidwell, S.M. and Barber, R.F., 2016. Inferring skeletal production from  
667 time-averaged assemblages: skeletal loss pulls the timing of production pulses towards the  
668 modern period. *Paleobiology*, 42, 54-76.

669 Tomašových, A., Kidwell, S.M. and Dai, R., 2023. A downcore increase in time averaging is  
670 the null expectation from the transit of death assemblages through a mixed layer.  
671 *Paleobiology*, 49, 527-562.

672 Tsujimoto, A., Yasuhara, M., Nomura, R., Yamazaki, H., Sampei, Y., Hirose, K. and  
673 Yoshikawa, S., 2008. Development of modern benthic ecosystems in eutrophic coastal  
674 oceans: the foraminiferal record over the last 200 years, Osaka Bay, Japan. *Marine*  
675 *Micropaleontology*, 69, 225-239.

676 Tumbiolo, M.L. and Downing, J.A., 1994. An empirical model for the prediction of secondary  
677 production in marine benthic invertebrate populations. *Marine Ecology Progress Series*, 114,  
678 165-174.

679 van der Plas, F., 2019. Biodiversity and ecosystem functioning in naturally assembled  
680 communities. *Biological Reviews*, 94, 1220-1245.

681 van de Pol, M. and Wright, J., 2009. A simple method for distinguishing within-versus  
682 between-subject effects using mixed models. *Animal Behaviour*, 77, 753-758.

683 Warwick, R., 1986. A new method for detecting pollution effects on marine macrobenthic  
684 communities. *Marine Biology*, 92, 557-562.

685 Warwick, R.M. and Clarke, K.R., 1994. Relearning the ABC: taxonomic changes and  
686 abundance/biomass relationships in disturbed benthic communities. *Marine Biology*, 118,  
687 739-744.

688 White, E.P., Adler, P.B., Lauenroth, W.K., Gill, R.A., Greenberg, D., Kaufman, D.M.,  
689 Rassweiler, A., Rusak, J.A., Smith, M.D., Steinbeck, J.R., Waide, R.B. and Yao J. 2006. A  
690 comparison of the species–time relationship across ecosystems and taxonomic  
691 groups. *Oikos*, 112, 185-195.

692 Wittmer, J.M., Dexter, T.A., Scarponi, D., Amorosi, A. and Kowalewski, M., 2014.  
693 Quantitative bathymetric models for late Quaternary transgressive-regressive cycles of the Po  
694 Plain, Italy. *Journal of Geology*, 122, 649-670.

695 Zimmt, J.B., Kidwell, S.M., Lockwood, R. and Thirlwall, M., 2022. Strontium isotope  
696 stratigraphy reveals 100 ky-scale condensation, beveling, and internal shingling of  
697 transgressive shell beds in the Maryland Miocene. *Palaios*, 37, 553-573.

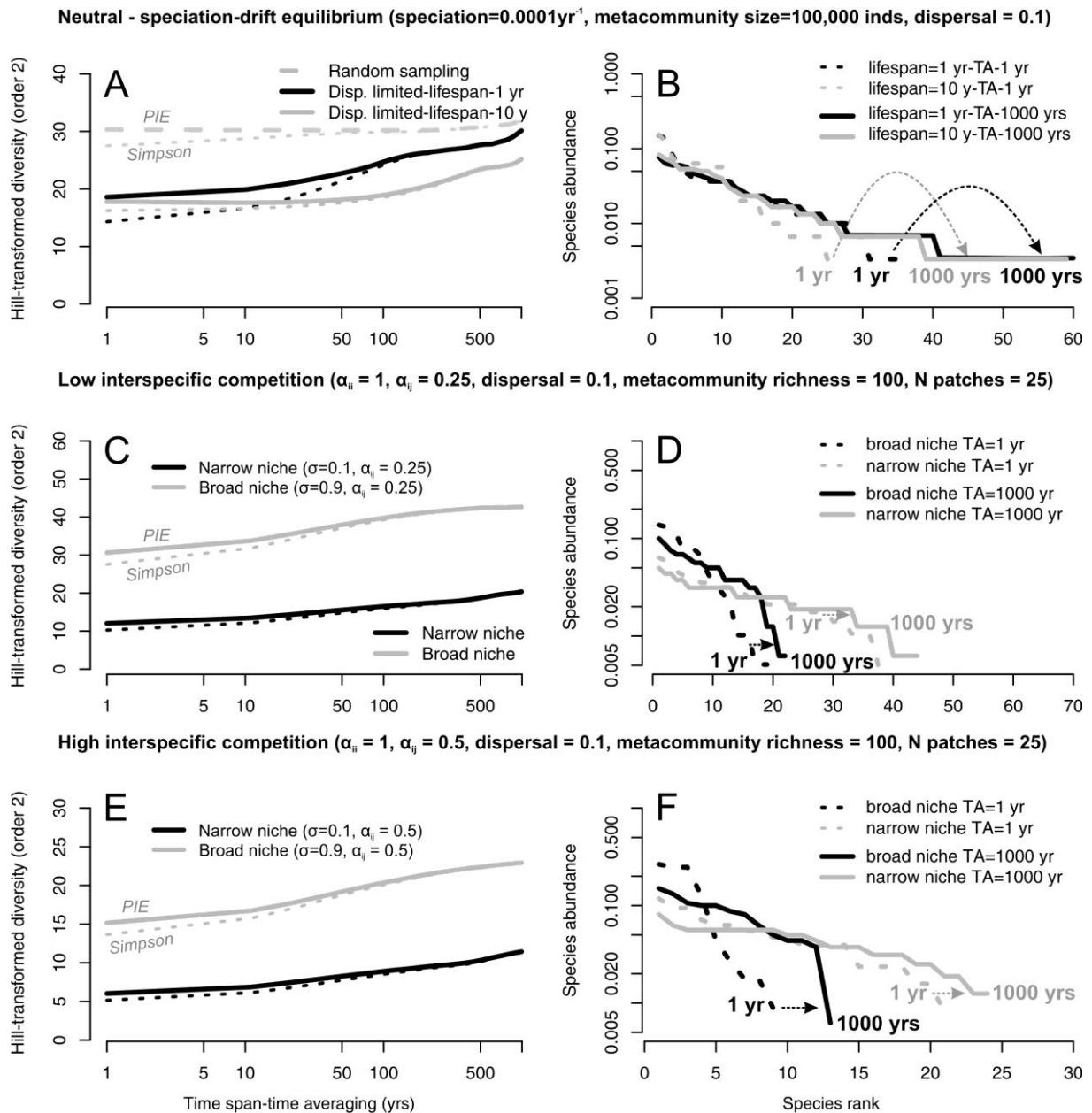
698

699

Response Predictor	Diversity (saturated model)	Diversity (abundance effect omitted)	Diversity (sediment accumulation effect omitted)	Diversity affected by abundance only ADR/ (unconditional)	Diversity affected by sedim. accumulation only	Abundance affected by sedim. accumulation and water depth	Abundance affected by sedim. accumulation only	Abundance affected by water depth only
Water depth (inverse of energy avail.)	0.323 s.e.=0.020 p=<0.001	0.32 s.e.=0.020 p=<0.001	0.333 s.e.=0.020 p=<0.001			0.018 s.e.=0.019 p=0.32		0.031 s.e.=0.021 p=0.14
Within-core sediment accumulation	0.002 s.e.=0.013 p=0.891	0.003 s.e.=0.013 p=0.78			-0.012 s.e.=0.016 p=0.462	-0.009 s.e.=0.010 p=0.39	-0.01 s.e.=0.010 p=0.324	
Between-core sediment accumulation	-0.242 s.e.=0.056 p=<0.001	-0.276 s.e.=0.040 p=<0.001			-0.343 s.e.=0.081 p=<0.001	-0.186 s.e.=0.046 p=<0.001	-0.193 s.e.=0.046 p=<0.001	
Within-core abundance	-0.026 s.e.=0.012 p=0.029		-0.023 s.e.=0.012 p=0.029	-0.019 s.e.=0.016 p=0.26				
Between-core abundance	0.15 s.e.=0.184 p=0.423		0.73 s.e.=0.15 p=<0.001	0.72 s.e.=0.31 p=0.028				
AIC	-3244.6	-3242.7	-3234.4	-3094.2	-3095	-3599.1	-3600.2	-3589.4
ΔAIC	0	1.9	12.1	150.4	149.6	1.05	0	9.7
Figure	4G	4G	4C, 4F	4E	3D	4G	3A	4C, 4F

700 **Table 1** – Summary statistics of linear mixed-effect models describing a relationship between  
701 sediment accumulation, water depth (inverse of energy availability), fossil diversity and  
702 abundance (visualized in figures specified on the bottom of the table). The coefficient (effect  
703 size), its standard error and p-values are shown for each predictor. Sediment accumulation and  
704 abundance are partitioned into within- and between-core components. The effect of between-  
705 core abundance on diversity is unconditionally positive or positive when conditioned on the

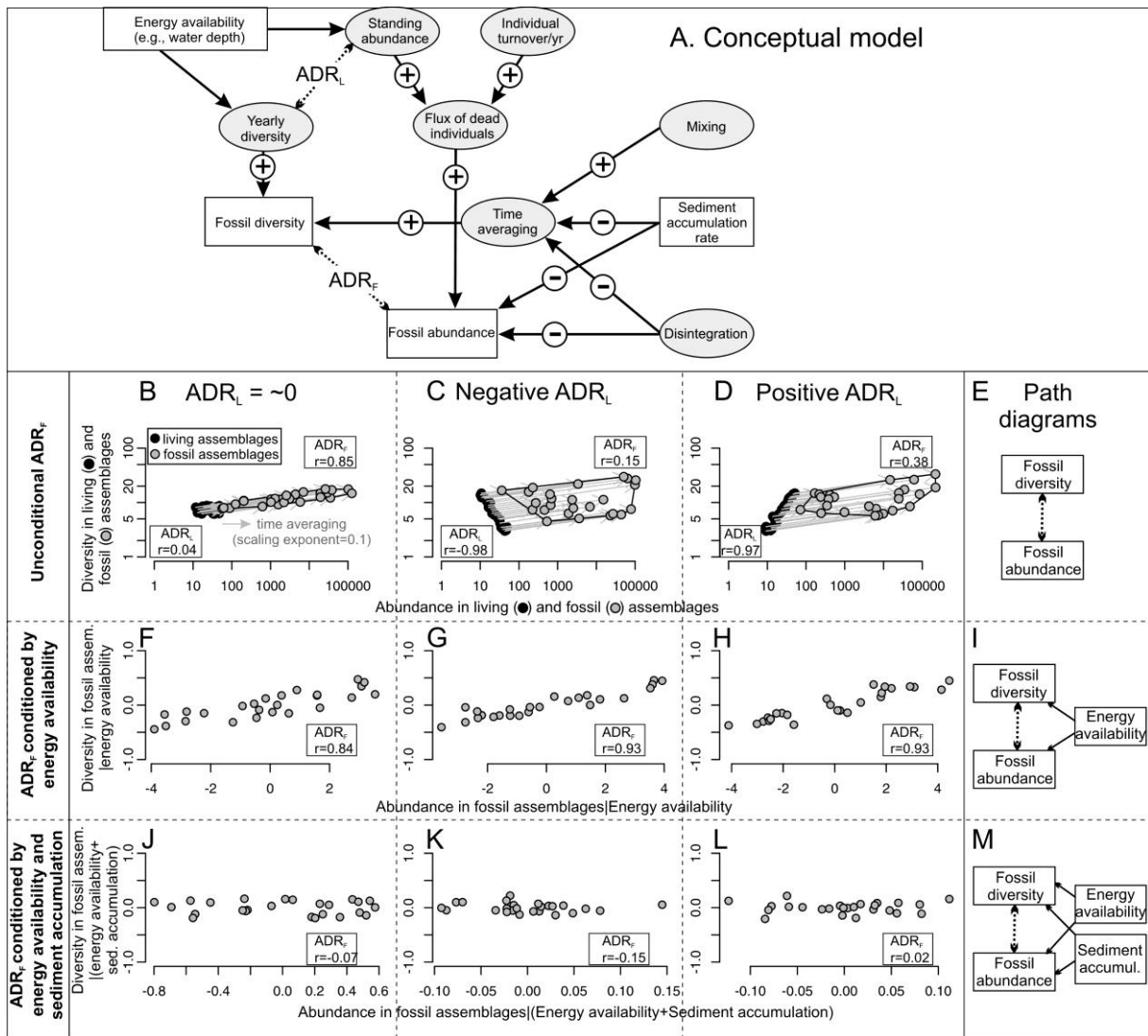
706 water depth but becomes insignificant when conditioned also on between-core sediment  
707 accumulation.



708

709 **Figure 1.** The conceptual figures visualizing the dependency of species diversity on timespan  
 710 of observation (species-time relationship) that flattens rank-abundance distributions and  
 711 ultimately leads to positive abundance-diversity relationship. The results are based on  
 712 outputs from two standard metacommunity models, including (A-B) neutral, spatially-implicit  
 713 metacommunity dynamics not limited (dashed gray) and limited by dispersal (solid black and  
 714 gray) and (C-F) non-neutral, spatially-explicit, dispersal-limited metacommunity dynamics  
 715 differing in species niche breadths ( $\sigma$ ) and in the strength of interspecific competition ( $\alpha_{ij}$ ).  
 716 Diversity is defined based on Hill-transformed diversity of order 2, using Simpson diversity  
 717 (dotted) and PIE-based diversity (solid). The PIE-based diversity remains constant when the  
 718 neutral dynamic is not limited by dispersal (gray dashed line in A). In this scenario, no

719 temporal scaling of diversity occurs because when the metacommunity pool is randomly  
720 sampled by the local community, the rank-abundance distribution does not change in shape  
721 with increasing time averaging. In all other scenarios, both neutral or non-neutral variants,  
722 any increase in the PIE-based diversity with increasing time averaging is associated with a  
723 decline in the species dominance and in the slope of the rank-abundance distribution as shown  
724 in the right column, where time averaging increases from 1 year (solid line) to 1000 years  
725 (dashed line). Non-averaged and time-averaged rank abundance distributions in each scenario  
726 are rarefied to the same sample size ( $n = 300$  individuals in neutral and 150 individuals in  
727 non-neutral models). The speciation timescale is 10,000 years and thus exceeds the maximum  
728 time averaging. If time averaging attains speciation timescale, diversity will exponentially  
729 increase in logarithmic space. The construction of species-time relationship follows a moving  
730 window approach of White et al. (2006). The simulations of neutral model are based on  
731 Hubbell (2001) and the simulations of non-neutral models follow Thompson et al. (2020),  
732 with R scripts in the Supplement.



734

735 **Figure 2.** The conceptual path diagram visualizing the variables that affect the abundance-736 diversity relation in living ( $ADR_L$ ) and in time-averaged fossil assemblages ( $ADR_F$ ) as

737 informed by generalized fossilization models (Tomašových et al. 2023). The nine cartoons

738 and three path diagrams exemplify the combined effect of  $ADR_L$  and time averaging on739  $ADR_F$ . (A) The conceptual path diagram. The white boxes represent the variables directly

740 measured or approximated in the fossil record. The gray ellipses visualize the variables not

741 directly measured in our dataset with fossil assemblages. Not all links are specified

742 exhaustively (e.g., sediment accumulation can negatively affect diversity or standing

743 abundance of living assemblage and fossil abundance can positively affect standing

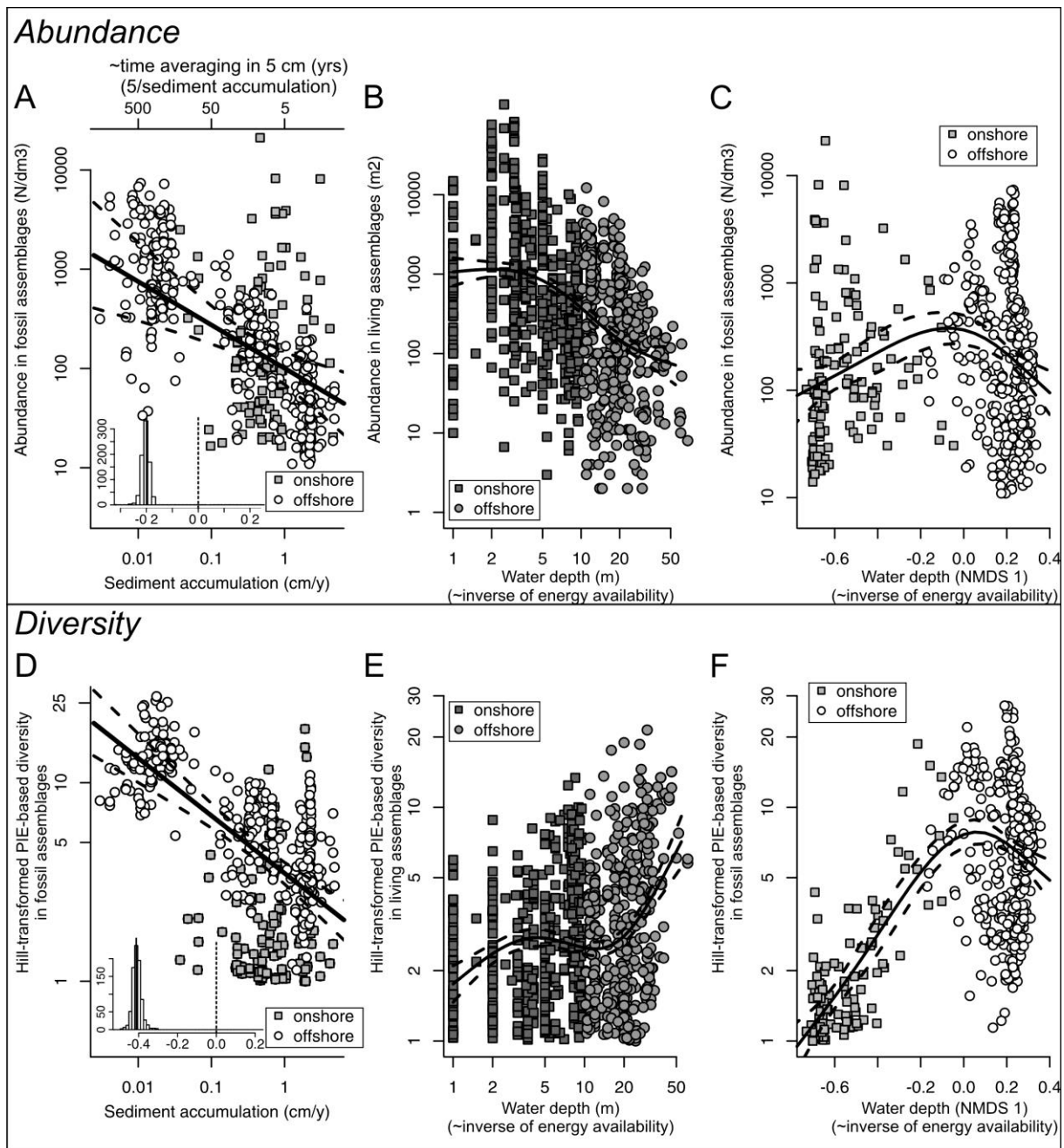
744 abundance of living assemblage and fossil abundance via taphonomic feedback). Energy availability can shape both abundance and

745 diversity of living assemblages, and thus determines  $ADR_L$ . (B-M) Conceptual cartoons746 visualizing three types of  $ADR_L$  patterns (with random, negative and positive  $ADR_L$  in three

747 columns) and three levels of conditioning (with unconditional  $ADR_F$  in B-D,  $ADR_F$   
748 conditioned on energy availability in F-I, and  $ADR_F$  conditioned on energy availability and  
749 sediment accumulation in J-M). 25 fossil assemblages are subjected to random time averaging  
750 (sampled from a uniform distribution delimited by 3 and 3000 years) and zero disintegration,  
751 the STR exponent is 0.1, and gray arrows correspond to the scaling expected under time  
752 averaging. Time averaging pulls the ADR of fossil assemblages (gray circles) towards  
753 positive values (upper row), although the sign of the unconditional  $ADR_F$  depends on the  
754 initial configuration of living assemblages (black circles). When the  $ADR_L$  is  $\sim 0$  (B), the  
755 unconditional  $ADR_F$  will be positive owing to the scaling effect. When the  $ADR_L$  is negative  
756 (C), the unconditional  $ADR_F$  will be less negative, but the scaling effect is cancelled out by  
757 the negative sign of the  $ADR_L$ . When the  $ADR_L$  is positive (D), the unconditional  $ADR_F$  will  
758 remain positive, regardless of the scaling effect. The positive effect of time averaging on  
759 abundance and diversity emerges in all scenarios when the  $ADR_F$  is conditioned on the  
760 ecological variable (e.g., energy availability) that forces the negative or positive  $ADR_L$  (F-H).  
761 Such positive  $ADR_F$  disappears when conditioned on the energy availability *and* sediment  
762 accumulation (J-L), providing a key insight into the contribution of time averaging to  
763 variability in fossil abundance and diversity. The path diagrams corresponding to each row  
764 are shown in the right column.

765



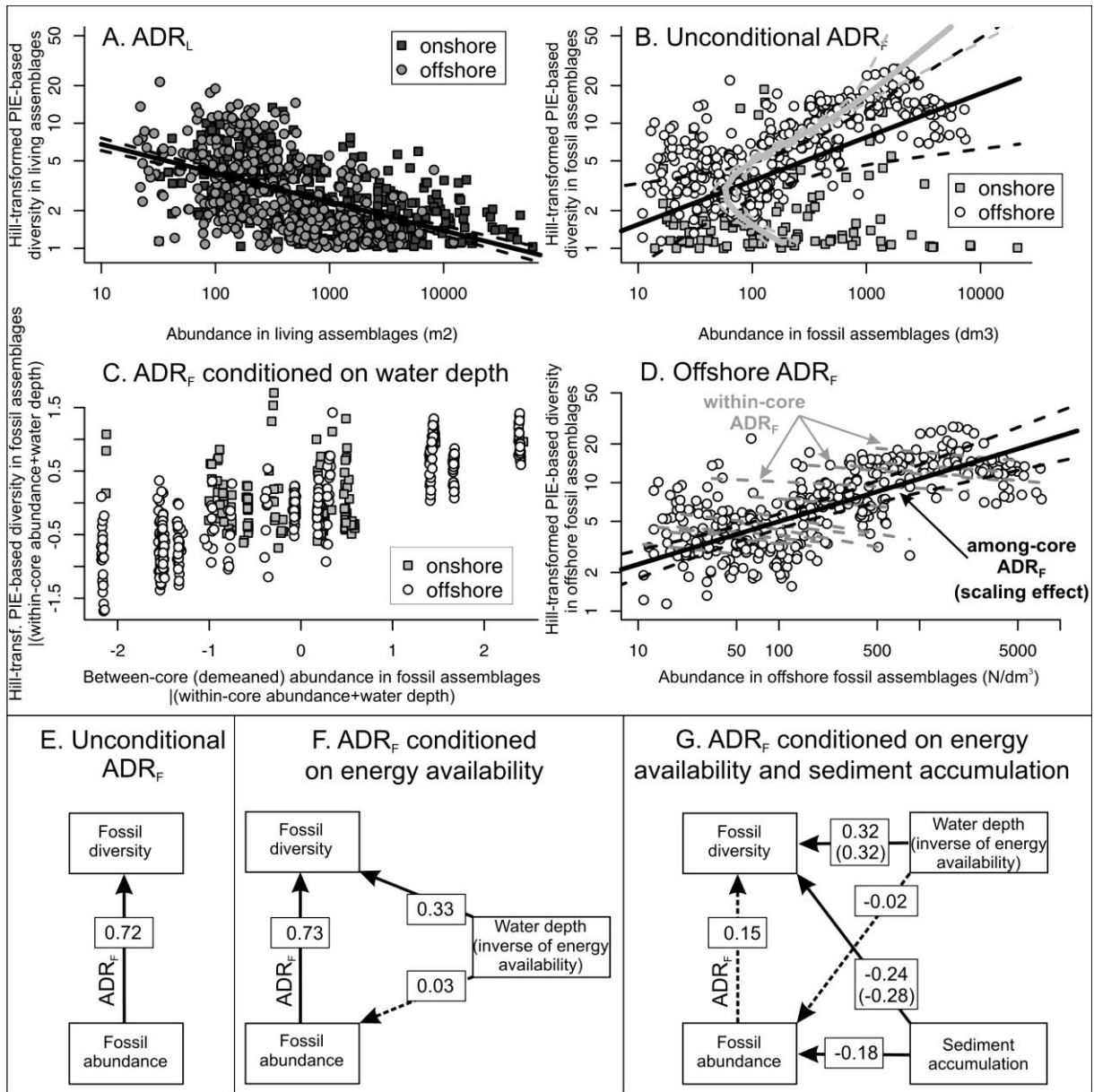


766

767 **Figure 3.** Sediment accumulation covaries negatively both with the abundance and diversity  
 768 of fossil assemblages as predicted by the scaling effects of time averaging on both variables  
 769 (via the species-time relationship). Sediment accumulation affects negatively both abundance  
 770 (A) and PIE-based diversity (D) in fossil assemblages (time averaging on the top axis  
 771 corresponds to the inverse of sediment accumulation, neglecting the thickness of the mixed  
 772 layer). Abundance declines with water depth (B), whereas the PIE-based diversity increases  
 773 with water depth (E) in living (non-averaged) assemblages. Abundance does not covary with  
 774 water depth (C), and the PIE-based diversity increases with water depth in time-averaged  
 775 fossil assemblages (F). Abundance~accumulation and diversity~accumulation relations in A

776 and D are estimated with the linear mixed-effect models (Table 1). The bathymetric gradients  
777 in abundance and diversity in living and fossil assemblages in B-C and E-F are fitted with  
778 generalized additive models (with 95% confidence intervals). The insets with frequency  
779 distributions capture negative effects of the effects of sediment accumulation on abundance  
780 (A) and diversity (D), based on the resampling of posterior estimates of sediment  
781 accumulation from Bayesian age-depth models. Note:  $N/dm^3$  – number of individuals in fossil  
782 assemblages per sediment volume. Source data: Table S1-S2.

783



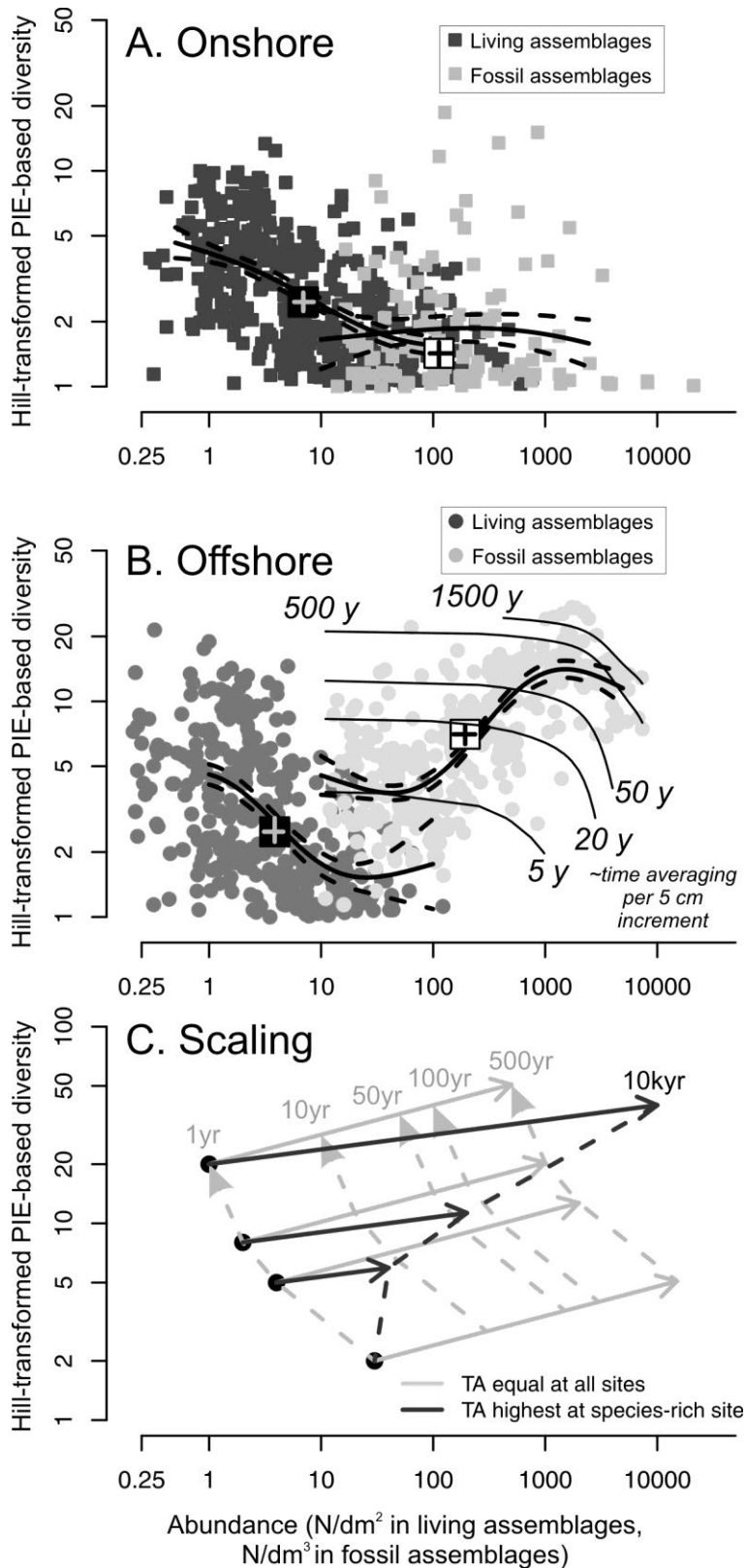
784

785 **Figure 4.** ADR is pulled towards the positive values as living assemblages are transformed  
 786 into fossil assemblages as predicted by the hypotheses postulating the effects of time  
 787 averaging (via sediment accumulation) on fossil abundance and diversity, and becomes  
 788 insignificant when conditioned on sediment accumulation. Raw (unconditional) ADR is  
 789 negative in living assemblages (A) and positive in fossil assemblages (B), and  $ADR_F$  remains  
 790 positive when conditioned on the water depth (C-D). The black lines represent the fit by the  
 791 generalized least-square model (with spherical correlation structure) in the  $ADR_L$  (A) and by  
 792 the linear mixed-effect model (cores as random effects and temporal autocorrelation modelled  
 793 by the autoregressive process of order 1) in the  $ADR_F$  (B). The gray lines in B correspond to  
 794 the U-shaped fit to the  $ADR_F$  by the generalized additive model. This  $ADR_F$  pattern

795 represents a trace of the scaling pathway that pulled offshore assemblages (with low diversity  
796 and low abundances) towards high fossil abundance and diversity. (C) Positive  $ADR_F$   
797 conditioned on the water depth, with residuals of between-core abundance effect on the x axis  
798 and diversity residuals on the y axis. (D) Focusing just on offshore assemblages allows for  
799 plotting the actual abundances and diversities rather than their residuals. The linear mixed-  
800 effect model with random slopes and intercepts visualizes that within-core  $ADR_F$  tends to be  
801 negative whereas the between-core effect of abundance on diversity is markedly positive. (E-  
802 G) Path diagrams visualizing the positive relation between fossil abundance and diversity  
803 (unconditional  $ADR_F$ , E), the  $ADR_F$  remains positive when conditioned on the water depth  
804 (F), and the  $ADR_F$  disappears when conditioned on the water depth and sediment  
805 accumulation (G) on the basis of 489 fossil assemblages in the Adriatic Sea. The numbers in  
806 white boxes represent standardized regression coefficients from linear mixed-effect models  
807 (with abundance and sediment accumulation effects corresponding to the between-core effects  
808 in Table 1), the dashed links reflect insignificant paths. The numbers in parentheses in G refer  
809 to the model where the effect of abundance on diversity is set to zero. Source data: Table S1-  
810 S2.

811

812



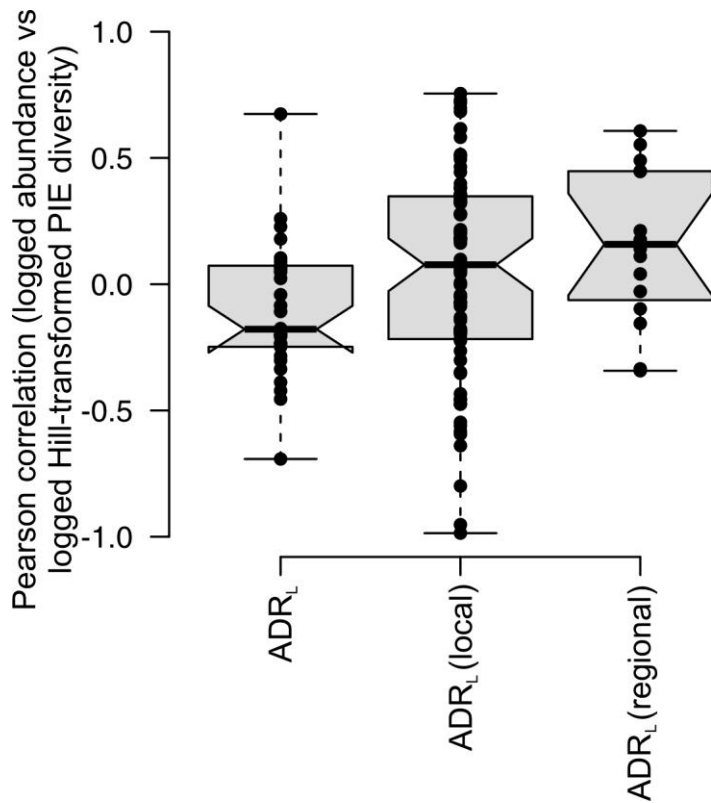
813

814 **Figure 5.** Reconstructing the scaling pathway leading from the negative  $ADR_L$  to the positive  
 815  $ADR_F$  by embedding living and fossil assemblages in the same abundance-diversity space.  
 816 The small differences in abundance and diversity between living (black) and fossil

817 assemblages (gray) in onshore environments with high sediment accumulation ( $>0.1$  cm/y)  
818 and thus very low time averaging (A) contrast with the ladder-like progression of abundance  
819 and diversity in offshore environments (B), where sediment accumulation is lower than 0.1  
820 cm/y and more variable, leading to the positive  $ADR_F$ . The contours correspond to  
821 approximate time averaging (in years) in 5 cm-increments (the inverse of sediment  
822 accumulation in years/cm multiplied by 5), fitted by generalized additive models. The boxes  
823 show mean abundance and diversity values with 95% bootstrapped confidence intervals. (C)  
824 The abundance shift along the x-axis depends on the sediment accumulation, assuming no  
825 disintegration and the diversity shift along the y-axis depends on the scaling slope of the  
826 species-time relationship (here, STR exponent is equal to 0.15, and all molluscs are assumed  
827 to have temporally-constant abundance and 1-year lifespan). The initial *local-scale*  $ADR_L$  is  
828 negative in non-averaged assemblages (four black circles, with poorly-diverse assemblages  
829 with high abundance and highly-diverse assemblages with low abundance). The shift towards  
830 the positive (regional-scale)  $ADR_F$  is magnified when species-rich but individual-poor  
831 assemblages are more averaged (to 10 kyr) than species-poor and individual-rich  
832 assemblages, as observed in the northern Adriatic Sea (black arrows with STR exponent =  
833 0.1, with endpoints connected by the dashed black line). In the absence of variability in time  
834 averaging, the  $ADR_F$  will remain negative (dashed gray lines). In A and B, as the volume of  
835 fossil samples varies between  $\sim 0.8$ - $1.3$  dm<sup>3</sup>, we standardize densities in living assemblages to  
836 N/dm<sup>2</sup> in these order-of-magnitude analyses (Van Veen grabs used for sampling living  
837 assemblages penetrate to sediment depths of 5-15 cm and are thus similar to the thickness of  
838 core increments ranging between 4-10 cm). Source data: Table S1-S2.

839

840



841

842

843 **Figure 6.** The systematic difference in the sign of the ADR<sub>L</sub> and ADR<sub>F</sub> exhibited by benthic  
844 foraminifers can reflect the effect of variable time averaging, with 29% of local FDRs and  
845 50% of regional FDRs exhibiting significantly positive relation. The ADR<sub>L</sub> patterns estimated  
846 on the basis of spatial surveys (n=30) are on average slightly negative. The ADR<sub>F</sub> patterns are  
847 based on fossil assemblages observed in local stratigraphic series (n=73) and in regional  
848 spatio-temporal datasets with at least two cores (n=25). Data sources: Table S3 and S4.

849 **Supporting Information for**  
850 **Abundance-diversity relationship as a unique signature of temporal scaling**

851

852 Adam Tomašových\*, Michał Kowalewski, Rafał Nawrot, Daniele Scarponi, Martin Zuschin

853

854 \*Corresponding author: Adam Tomašových

855 **Email:** geoltoma@savba.sk

856

857 **This PDF file includes:**

858

859 Supporting text

860 Figures S1 to S11

861 Tables S1 to S5

862 SI references

863 Data files and scripts:

864 [https://datadryad.org/stash/share/dEfyOr0s3aBnuN3KMAloel-mi1eZ\\_Eg--fxyjlzszXM](https://datadryad.org/stash/share/dEfyOr0s3aBnuN3KMAloel-mi1eZ_Eg--fxyjlzszXM)

865

866

867

868

869

870



871 **Supporting text**

872

873 **Sampling.** The dataset with 1,150 living assemblages compiled from 27 studies (Figure S1,  
874 Table S1) is restricted to assemblages with a minimum size of 10 individuals. In some cases,  
875 it includes repeated bi-annual or annual sampling (such assemblages were not pooled to avoid  
876 analytical time averaging). The assessment of the abundance-diversity relationship is based on  
877 assemblages that were completely censused at the species level. Several surveys focused on  
878 estimating the abundance of the most common species (*Lentidium mediterraneum* or  
879 *Chamelea gallina*) in the shallowest habitats document extremely high population densities,  
880 exceeding 20,000-30,000 individuals/m<sup>2</sup>. Although they do not capture the sample total  
881 abundance (i.e., all molluscan individuals), we use these densities as minimum estimates of  
882 abundance in assessments of the depth-abundance relationship in Figure 3. Such incomplete  
883 samples that lack data on abundances of other species were excluded from other analyses of  
884 ADRs.

885         The 26 cores with 489 fossil assemblages span from siliciclastic deltaic settings with a  
886 high sediment accumulation rate (in the NW Adriatic Sea and in the Gulf of Trieste) to  
887 current-winnowed and sediment-starved, siliciclastic-carbonate settings with a low sediment  
888 accumulation rate (in the NE segment). The cores archive the recentmost centuries at sites  
889 with a high sediment accumulation rate (0.2-2 cm/y) or span ~9-10 kyr (corresponding to the  
890 flooding of the northern Adriatic shelf) at sites with low sediment accumulation rates (<0.02  
891 cm/y). These short cores were split into 4-5 cm-thick increments; assemblages from all  
892 increments were surveyed. Fifteen cores (> 10 m-long) from the Po coastal plain (deposited at  
893 ~ 1 cm/y during the highstand phase and at < 0.25 cm/y during the transgressive phase,  
894 Scarponi et al. 2013) were split into 5 and 10 cm increments that were sampled either at  
895 regular intervals separated by 1-3 m or more densely at intervals characterized by facies  
896 shifts. 489 fossil assemblages cover delta front (n=105), barrier island (n=32), transgressive  
897 sand sheet (n=68), prodelta (n=207), and offshore transition facies associations (n=78). Total  
898 abundance refers to the total number of uniquely identifiable specimens (with umbo or hinge  
899 preserved) and thus is not affected by differences in fragmentation among sites or increments.  
900 When sample sizes exceeded more than several thousands of individuals, increments were  
901 split into fractions and the fraction-level count was multiplied by the fraction inverse to derive

902 the total abundance per total increment volume (e.g. if half of the sample was processed, the  
903 total number of individuals was multiplied by two) (Gallmetzer et al. 2019).

904

905 ***Age models and sediment accumulation rates.*** Short and densely-sampled cores include  
906 M13, M14, M20 and M21 in the proximal parts of the Po prodelta, POS514-GC-25-5 in the  
907 distal parts of the Po prodelta, M28 and M29 in the Isonzo prodelta (Bay of Panzano), M38 in  
908 the current-winnowed Gulf of Venice, M1 and M53 at Piran, and M44 at Brijuni. Fifteen (>  
909 10 m-long) cores from the Po coastal plain include 240-S8, 205-S4, 205-S14, 205-S10, 205-  
910 S9, 205-S7, 204-S7, 205-S1, 205-S2, 256-S3, 205-S6, 204-EM-S5, 188-EM-S4, 187-EM-  
911 S12, and 187-C Goro. Sediment cores were sampled with two sampling strategies that partly  
912 differ in core length, core diameter and density of increment sampling. Age models were  
913 directly estimated for cores Po 3-M13, Po 4-M21, Panzano-M28, Piran-M53, and extrapolated  
914 to spatially-proximate cores Po 3-M14, Po 4-M20, Panzano-M29, and Piran-M1 with highly –  
915 similar lithological attributes and stratification patterns (Figure S3). In contrast to shorter  
916 piston and gravity cores, age models at the coastal Po Plain are based on a smaller number of  
917 age-dating levels (at least two dated levels per systems tract) (Figure S2). The core lithology  
918 and fossil molluscan assemblages in these cores were described previously (Scarponi and  
919 Kowalewski 2004, 2007; Kowalewski et al. 2015; Gallmetzer et al. 2017, 2019; Tomašových  
920 et al. 2018; Berensmeier et al. 2023).

921 The primary references for 26 cores are as follows: 240-S8 (Campo et al., 2020; Cheli  
922 et al., 2021), 205-S4 (Scarponi et al. 2013; Amorosi et al., 2017; 2020; 2021), 205-S14  
923 (Scarponi et al., 2013; Amorosi et al., 2017), 205-S10 (Sarti et al., 2009; Campo et al., 2020),  
924 205-S9 (Sarti et al., 2009; Bruno et al., 2017; Amorosi et al., 2020), 205-S7 (Cibin et al.,  
925 2005; Scarponi et al., 2013; Amorosi et al., 2017), 204-S7 (Calabrese et al., 2009; Amorosi et  
926 al., 2017; Bruno et al., 2019), 205-S1 (Amorosi et al., 2003; Sarti et al., 2009), 205-S2  
927 (Campo et al., 2020; Amorosi et al., 2021), 256-S3 (Severi et al., 2005; Campo et al., 2020),  
928 205-S6 (Sarti et al., 2009; Amorosi et al., 2017, 2020), 204-EM-S5 (Amorosi et al., 2017),  
929 204-EM-S4 (Amorosi et al., 2017), 188-EM-S5 (Amorosi et al., 2017), 187-EM-S12  
930 (Amorosi et al., 2017), 187-C\_Goro\_I (Sarti et al., 2009), Po 3 M13, Po 3 M14, Po 4 M20, Po  
931 4 M21 (Tomašových et al. 2018), Panzano M28 and M29 (Tomašových et al. 2017), Piran 1  
932 M1 and Piran 2 M53 (Mautner et al. 2018, Tomašových et al. 2019), Venice M38 (Gallmetzer  
933 et al. 2019), Brijuni M44 (Schnedl et al. 2018, Tomašových et al. 2022), and Poseidon core

934 POS514 – GC-25-5 (Berensmeier et al. 2023). The top-core age estimation of cores drilled at  
935 the Po Plain, which was a swampy area until a few decades or centuries ago, is based either  
936 on the year of final land reclamation of the area where the core was drilled (the cores 205-S1,  
937 205-S2; 204 EM-S5, and 188 EM-S5 were drilled in areas that were reclaimed in 1964 AD,  
938 the core 205-S6 was drilled in area reclaimed in 1919 AD, the core 205-S7 in area reclaimed  
939 in 1933 AD, and the core 205-S10 in area reclaimed in 1958 AD) or on the basis of  
940 information in geological maps and seismic profiles (Scarponi et al. 2013).

941 Bayesian age-depth models and sediment accumulation (cm/y) were estimated with  
942 the Bacon function (rbacon package, Blaauw and Christen 2011, Blaauw et al. 2021) on the  
943 basis of 1) single-shell radiocarbon estimates (with the mean age and age error represented by  
944 standard deviation based on the radiocarbon calibration), 2) amino-acid and radiocarbon  
945 estimates from multiple shells dated from the same core increment (with the mean of age  
946 distribution and its standard error; the spread of within-increment ages directly reflects natural  
947 time averaging of co-occurring shells as the measurement error is typically smaller than range  
948 of ages induced by slow sedimentation and high mixing in these cores, Scarponi et al. 2013;  
949 Tomašových et al. 2017, 2018, 2022), and 3) the timing of the boundary between the  
950 highstand systems tract and the maximum flooding zone constrained on the basis of seismic  
951 stratigraphy (~7,000 years BP, Amorosi et al. 2017). The calibration of amino acid and  
952 radiocarbon ages and among-core correlations are presented in the references cited in the  
953 previous paragraph, the input data for the Bacon function are listed in the Supplementary  
954 Table 6. The parameter of the prior beta distribution for autocorrelation among sediment  
955 accumulation rates within cores was set to a minimum dependency (mean=0.01) with shape =  
956 100 (corresponding to a small variance in memory). The prior beta distribution for sediment  
957 accumulation time (in years/cm) was set to the overall long-term sedimentation time (core  
958 duration/core thickness) and the shape parameter of the beta distribution was set to 0.5 (when  
959 core spanned several systems tracts) or 2 (when empirical age data do not indicate any major  
960 change in sediment accumulation rate).

961 Sediment accumulation rates based on age models in these cores are moderate to high  
962 (0.1-5 cm/y) in facies associations deposited in intertidal and upper shoreface environments.  
963 They are more variable in lower shoreface to offshore environments, ranging from very low  
964 (~0.001 cm/y) at locations affected by winnowing and sediment starvation to high (~5 cm/y)  
965 at deltaic settings (Figure S4-S5). This bathymetric decline in sediment accumulation is in

966 accord with modern, decadal-scale estimates in deltaic settings and with the bathymetric  
967 decline in sediment accumulation observed in the northern Adriatic Sea (Frignani and  
968 Langone 1991).

969         The effect of sediment accumulation on abundance and diversity or conditional  
970 independence between them may be assessed only when age models are based on a  
971 sufficiently high number of dated intervals. When based on a few dated intervals, the  
972 estimates of sediment accumulation rate will not resolve smaller-scale variability in  
973 sedimentation (and thus in time averaging) when interpolating sediment accumulation rates to  
974 undated levels. The estimates of sediment accumulation may be decoupled from time  
975 averaging, thus potentially also not tracking the true variability in time averaging, but  
976 Holocene fossil assemblages in the Adriatic Sea tend to show the close relation between  
977 residence times of molluscan remains in 5-10 cm-thick increments predicted on the basis of  
978 sediment accumulation and direct estimates of time averaging based on dating of at least ten  
979 shells per increment (Scarponi and Kowalewski 2013, Tomašových et al. 2022).

980         All analyses are performed with R Core Team (2021), version 4.3.0, including the  
981 following packages: nlme (Pinheiro et al. 2023), mgcv (Wood 2011), vegan (Oksanen et al.  
982 2020), datawizard (Patil et al. 2020), AICcmoavg (Mazerolle et al. 2023), truncnorm  
983 (Mesmann et al. 2018), iNEXT (Hsieh et al. 2016), piecewiseSEM (Lefcheck 2016),  
984 synchrony (Gouhier T.C. and Guichard 2014), dplyr (Wickham 2016), ggplot2 (Wickham  
985 2016), and rbacon (Blaauw and Christen 2011).

986

987 ***The species-time relationship (STR)***. The estimates of diversity that are independent of  
988 sample size, such as the PIE-based diversity or rarefied species richness, will not increase  
989 with increasing time averaging when assemblages are randomly assembled (not limited by  
990 dispersal) from metacommunities with temporally constant species-abundance distributions  
991 (gray dashed line in Figures 1A). This scenario is also directly equivalent to the random  
992 sampling model when an increase in species richness reflects increasing sampling from a  
993 static species pool (Coleman 1981). Therefore, except in rare scenarios where the temporal  
994 dynamic of assemblages is not limited by dispersal and local assemblages are random samples  
995 from the metacommunity that follows a random-walk dynamic (drift-diversification, Hubbell  
996 2001), diversity estimates based on sample size standardization do not correct for among-  
997 sample differences in time averaging. When the duration of the time series approaches the

998 time scale of species diversification, PIE-based diversity will increase with increasing time  
999 averaging even under a random metacommunity assembly.

1000         Once time averaging integrates across community assembly limited by dispersal or  
1001 driven by non-neutral dynamic, different values of time averaging will produce misleading  
1002 differences in diversity. We note that the scaling effect does not necessarily increase the  
1003 evenness measures that have species richness in the denominator because the sensitivity of  
1004 these indices to time averaging depends on the ratio of higher-order diversity relative to  
1005 species richness. For example, in the absence of immigration from other regions and/or when  
1006 turnover in species identity at the local scale is minor, species richness will increase with  
1007 time, averaging less than the diversity of order two, thus also increasing evenness. When  
1008 species richness increases with time averaging at a higher rate than the diversity of order two  
1009 owing to significant turnover in species identity (as can happen in neutral models), evenness  
1010 can decline with increasing time averaging.

1011

1012 ***Bathymetric gradients in diversity and abundance.*** We assess differences in abundance and  
1013 diversity between living and fossil assemblages within habitats by partitioning living  
1014 assemblages (shallower and deeper than 10 m) and fossil assemblages (defined by two main  
1015 groups of samples in the cluster analyses that correspond to the assemblages dominated by  
1016 *Lentidium* and *Chamelea* on the one hand and by species preferring offshore habitats on the  
1017 other hand) into two equivalent depth segments differing not only in exposure to salinity  
1018 fluctuations, in hydrodynamic conditions and grain size but also in community composition.  
1019 The Bray-Curtis and Hellinger distances generate equivalent clusters and NMDS ordination  
1020 patterns (Figure S6-S8). The shallower (onshore) assemblages are dominated by *Lentidium*  
1021 and *Chamelea* (inhabiting nearshore environments), and the deeper (offshore) assemblages by  
1022 *Varicorbula*, *Turritellinella*, *Timoclea* and *Gouldia* (thriving in offshore transition and  
1023 offshore environments). This categorization allows us to assess whether the abundance and  
1024 diversity of fossil assemblages exceed those of living assemblages, as predicted by the R-  
1025 sediment model (Kidwell 1986), and to approximate how the  $ADR_F$  is shaped by time  
1026 averaging while controlling for differences related to bathymetry. The analyses based on the  
1027 relationship between the Hill-transformed sample size-corrected Shannon diversity (Chao et  
1028 al. 2014), fossil abundance, and sediment accumulation generate almost identical results. In

1029 our datasets, the PIE-based diversity also correlates strongly with Pielou's J in living (r =  
1030 0.85,  $p < 0.0001$ ) and fossil assemblages ( $r = 0.91$ ,  $p < 0.0001$ ).

1031 As the positive FADR patterns are predicted to be observed when fossil assemblages  
1032 form under different sediment accumulation, we primarily focus on the regional-scale ADR  
1033 (observed in assemblages collected in multiple sediment cores that capture larger bathymetric  
1034 and geographic gradients or cover longer temporal extents than individual sediment cores) in  
1035 our analyses of fossil assemblages in the northern Adriatic Sea, although we also report the  
1036 local-scale  $ADR_F$  (observed in individual sediment cores). The mean abundance of living  
1037 assemblages declines from 4,730 at depths  $< 5$  m to 853 at 10-20 m and to 243 at depths  $> 20$   
1038 m. Fossil assemblages preserved in offshore environments are on average equally rich in  
1039 individuals as those from onshore environments, with mean abundance equal to 650-750  
1040 individuals/dm<sup>3</sup> on both sides of the ordination gradient. The mean PIE-based diversity  
1041 increases with depth both in living assemblages ( $r = 0.22$ ,  $p < 0.0001$ ) by a factor of ~2-3,  
1042 from 3.1 at depths  $< 10$  m to 3.2 at 10-20 m and 4.6 at depths  $> 20$  m and in fossil  
1043 assemblages ( $r = 0.68$ ,  $p = < 0.0001$ ). The PIE-based diversity of fossil assemblages increases  
1044 by a factor of ~3 when comparing onshore and offshore environments (from 2.7 in  
1045 assemblages with negative scores to 8.4 in assemblages with positive scores), parallel with  
1046 declining sediment accumulation. However, the diversity of fossil assemblages in offshore  
1047 environments is variable, ranging from almost monospecific assemblages up to highly diverse  
1048 assemblages with  $> 20$  equally abundant species. The bathymetric decline in the dominance  
1049 structure in fossil assemblages parallels the increase in evenness ( $r$  [Pielou's J] = 0.7,  $p <$   
1050 0.0001). The Hill-transformed Shannon diversity gives similar results as PIE-based diversity.  
1051 The correlation between sediment accumulation and PIE-based diversity is negative when the  
1052 effect of abundance is factored out. The diversity of individual-rich fossil assemblages (with  
1053 more than 250 individuals/dm<sup>3</sup>) is bimodally-distributed, whereas the diversity of individual-  
1054 poor fossil assemblages ( $< 250$  individuals/dm<sup>3</sup>) is distributed uniformly or unimodally.

1055

1056 **Structural equation models.** In parallel with the linear mixed-effect models, we also use  
1057 structural equation models (SEM, Schumacker and Lomax 2010) to assess whether a decline  
1058 in sediment accumulation increases the abundance and diversity of fossil assemblages and at  
1059 the same time accounts for the positive effects of abundance on diversity if conditioned by  
1060 sediment accumulation. Although this simple approach does not incorporate temporal

1061 autocorrelation and heterogeneity among cores, the among-variable relationships directly  
1062 parallel the setup of linear mixed-effect models. The saturated model ( $df=0$ ) is compared with  
1063 a reduced model without any unique effect of abundance on diversity on the basis of the  
1064 Akaike information criterion and on the basis of the likelihood-ratio Chi-square statistic. The  
1065 full model visualized in Figure 2B ( $AIC = 4182.9$ ) explains 48% of the variation in fossil  
1066 abundance by variability in sediment accumulation and water depth and 74% of the variation  
1067 in diversity by variability in sediment accumulation, water depth, and fossil abundance. All  
1068 paths are significant at  $p < 0.05$ , except for the effect of depth on abundance ( $p = 0.2$ ) and  
1069 abundance on diversity ( $p = 0.18$ ). 74% of the variation in diversity is also explained by  
1070 variability in sediment accumulation and water depth in the model where the covariance  
1071 between fossil abundance and fossil diversity is set to zero ( $AIC = 4183.2$ , likelihood-ratio  
1072 test  $\chi^2 = 1.77$ ,  $p = 0.18$ ). The unconditional positive covariance between the abundance and  
1073 diversity of fossil assemblages is thus entirely accounted for by the effect of the sediment  
1074 accumulation.

1075

1076 ***Abundance-diversity relation in molluscan fossil assemblages.*** The frequency and the  
1077 strength of the  $ADR_F$  in the stratigraphic record depends on the LADR (Figure 2A-C), on  
1078 disintegration and mixing processes, on variability in time averaging, and on the magnitude of  
1079 the slope of the STR, and is thus difficult to predict. The raw  $ADR_F$  exhibiting the U-shaped  
1080 pattern reflects the complex interaction between the negative  $ADR_L$  and the time averaging  
1081 effect pulling the abundance-diversity relation towards positive values (Figure 4B). When the  
1082  $ADR_L$  is not random and rather negative, as in the northern Adriatic Sea, conditioning the  
1083  $ADR_F$  on the main variable that covaries with the  $ADR_L$  (water depth) leads to a strongly  
1084 positive relationship (Figure 4C-D). We note that in a scenario where the scaling exponent of  
1085 the STR increases with depth but time averaging is equally high at all depths, offshore  
1086 assemblages will be more diverse than onshore assemblages but not more rich in individuals.  
1087 Therefore, the bathymetric shift in the STR slope alone, not associated with variability in time  
1088 averaging, is not sufficient to generate the abundance-diversity relation.

1089 In any case, the positive  $ADR_F$  can primarily emerge when abundance and diversity  
1090 patterns are assessed in stratigraphic successions deposited under variable sediment  
1091 accumulation.  $ADR_F$  patterns within individual cores in our Adriatic dataset are rarely  
1092 significantly positive because most are characterized by a limited variability in sediment

1093 accumulation and fossil abundance. Simple Pearson correlations observed within individual  
1094 cores are highly variable, ranging between -0.7 and 0.63 (with significantly positive value  
1095 observed in one core only). 13 out of 20 cores exhibit a range of time averaging values among  
1096 5-10 cm increments that are smaller than 50 years, approximated on the basis of the inverse of  
1097 sediment accumulation. The strongly positive  $ADR_F$  emerges in regional-scale analysis only  
1098 when assemblages within cores are time-averaged to varying degrees. Similarly, although the  
1099 microfossil records show the positive  $ADR_F$  also at the scale of individual cores, the  
1100 proportion of datasets with significantly positive  $ADR_F$  patterns increases to 50% when  
1101 assessed at regional scales spanning multiple cores.

1102

1103 ***Microfaunal records.*** Our criteria used in the selection of time series with fossil assemblages  
1104 from the Marben subset of the Biodeeptime database include explicit information on volume-  
1105 or mass-standardized estimates of per-assemblage total abundance, complete species-level  
1106 census abundance counts not excluding any rare species, at least ten samples with quantitative  
1107 abundance data per time series, and the associated age model. We assessed the frequency of  
1108 the significantly positive  $ADR_F$  patterns at the scale of individual cores (73 datasets) and at  
1109 the scale of larger regions that consist of at least two cores (25 datasets). These datasets span  
1110 five orders of magnitude in duration, from 10 years to more than 100,000 years. However, we  
1111 also assessed the frequency of cores with a significantly positive  $ADR_F$  relative to the total  
1112 number of cores in settings where the preconditions for a significantly positive  $ADR_F$  are met.  
1113 For this purpose, we exclude the cores with low variability in time averaging and abundance  
1114 in a subset of analyses focused on individual sediment cores. We use these three criteria to  
1115 select this subset of cores - coefficients of variation in time averaging and in fossil abundance  
1116 across the cores exceed 0.25 (i.e., time averaging and fossil abundance vary by more than  
1117 25% relative to the mean abundance) and mean sediment accumulation rates are not high  
1118 (with mean sediment accumulation smaller than 0.2 cm/y). When computing the coefficient of  
1119 variation in time averaging between all adjacent assemblages in each core or region, we use  
1120 an inverse of the sediment accumulation as a proxy for time averaging (ignoring the depth of  
1121 the mixed layer). The generalized least-square models that account for temporal  
1122 autocorrelation (with the same structure as in the mixed-effect models) return a similar  
1123 frequency of significantly positive  $ADR_F$  patterns for individual time series.

1124



1125           ***Effects of disintegration and false negatives.*** The increase in fossil abundance driven  
1126 by the lack of dilution can be counteracted by the disintegration of skeletal remains.  
1127 Disintegration can reduce the abundance of dead individuals accumulating in the surface  
1128 mixed layer to below the standing abundance of their source living assemblage (Kidwell  
1129 2002). Post-mortem age-frequency distributions indicate that the disintegration of molluscan  
1130 remains occurs on decadal scales in the northern Adriatic Sea (Tomašových et al., 2022).  
1131 Therefore, fossil abundances observed in this setting are expected to be smaller relative to  
1132 scenarios where disintegration is slower or can be neglected. However, the fossil abundance  
1133 in the core samples (mean = 730 N/dm<sup>2</sup>, max = 7,400 N/dm<sup>2</sup>) exceeds the living abundance  
1134 observed in benthic surveys (mean = 6 N/dm<sup>2</sup>, max = 122 N/dm<sup>2</sup>) by more than two orders of  
1135 magnitude in offshore environments. Therefore, the effect of disintegration does not cancel  
1136 out the negative relation between fossil abundance and sediment accumulation. In onshore  
1137 environments, the mean fossil abundance (mean = 650 N/dm<sup>2</sup>, max = 21,000 N/dm<sup>2</sup>) exceeds  
1138 the mean living abundance (mean = 50 N/dm<sup>2</sup>, max = 1,370 N/dm<sup>2</sup>) by a smaller factor than  
1139 in offshore environments, probably reflecting the effect of higher dilution of molluscan  
1140 remains by clastic sediments.

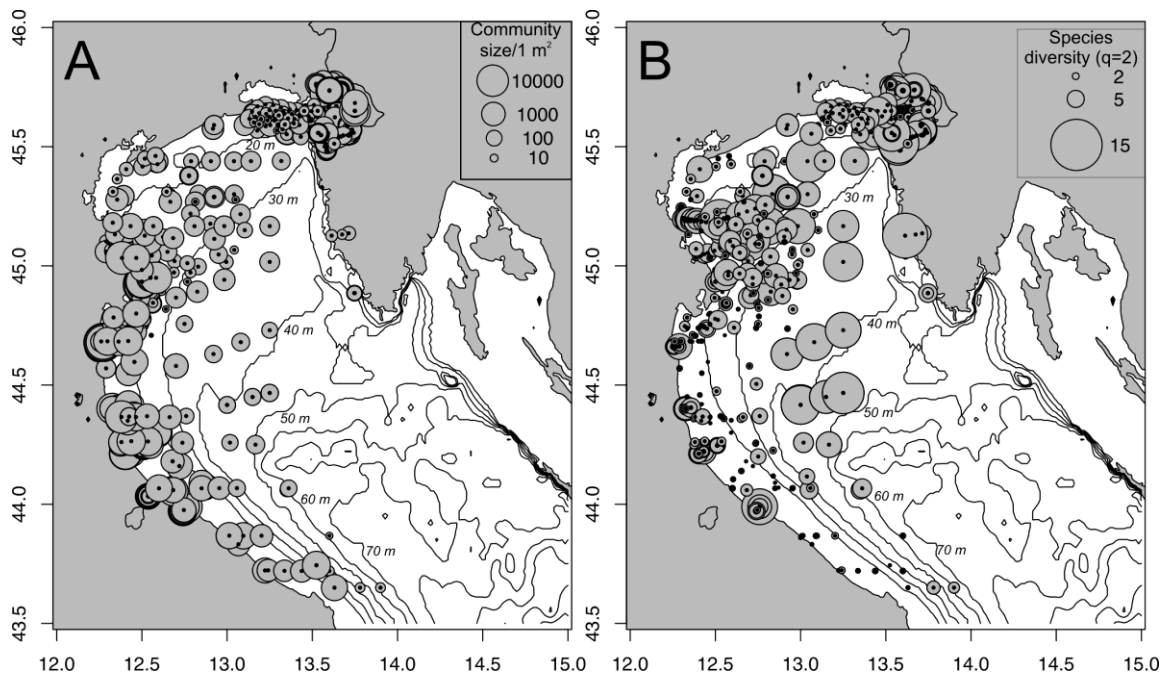
1141           In general, the positive ADR<sub>F</sub> can be a conservative criterion of the temporal scaling  
1142 effect owing to the potential for false negatives. Even when fossil remains disintegrate  
1143 rapidly, stochastic mixing by burrowers can still allow some remains to be buried into the  
1144 historical layers and thus will be incorporated into the stratigraphic record. This dynamic can  
1145 lead to highly time-averaged but shell-poor assemblages (Tomašových et al. 2023), leading to  
1146 no differences in fossil abundance between weakly-averaged assemblages with lower  
1147 diversity and highly time-averaged assemblages with higher diversity. The scenario where  
1148 time averaging does not covary with fossil abundance can thus generate false negative results  
1149 concerning the role of time averaging even when diversity differences among fossil  
1150 assemblages are triggered by differences in time averaging.

1151

1152           ***Role of anthropogenic impacts.*** Both abundance and diversity of living assemblages  
1153 collected in the late 20th and in the 21st century can be negatively affected by anthropogenic  
1154 impacts, thus magnifying the differences between non-averaged living assemblages and time-  
1155 averaged fossil assemblages or artificially contributing to the positive ADR<sub>F</sub> (e.g., when some  
1156 weakly time-averaged assemblages have low diversity because they were sourced by

1157 impacted communities over the past decades). First, excluding the Anthropocene samples  
1158 (typically represented by assemblages sourced by communities in the 20th century and  
1159 located in the upper 20 cm of sediment cores, exceptionally in the upper 90 cm at Po Delta)  
1160 also generates a significantly positive  $ADR_F$  in the whole northern Adriatic Sea ( $r = 0.46$ ,  $p <$   
1161  $0.0001$ ) and also within offshore environments ( $r = 0.71$ ,  $p < 0.0001$ ). Second, the disparity in  
1162 abundance between fossil and living assemblages driven by time averaging can be biased up  
1163 because abundances of some molluscan species and the overall molluscan production have  
1164 been depressed over the last century owing to anthropogenic eutrophication, hypoxia,  
1165 trawling, or pollution relative to the earlier Holocene conditions (Haselmair et al. 2021).  
1166 However, the 20<sup>th</sup>-century decline in molluscan population densities is probably not sufficient  
1167 to generate the order-of-magnitude increase in abundance in time-averaged fossil assemblages  
1168 relative to their living counterparts.

1169



1170

1171

1172 **Figure S1.** Geographic distribution of living molluscan assemblages analyzed in this study  
 1173 visualizes the negative relation between the standing abundance of molluscs and their  
 1174 diversity in the northern Adriatic Sea. A. Total molluscan abundance in living assemblages  
 1175 (individuals/m<sup>2</sup>) tends to decline with increasing water depth. B. The Hill-transformed PIE-  
 1176 based diversity of living assemblages tends to increase with increasing water depth. Data  
 1177 sources for assemblages collected alive: Ambrogi and Ambrogi 1985, Ambrogi et al. 1995,  
 1178 ARPAAE 2010-2019, Chiantore et al. 2001, ENEA database, Forni et al. 2005, Haselmair et al.  
 1179 2021, ISPRA 2012, Mavric et al. 2010, Moodley et al. 1998, Nasi et al. 2020, N'Siala et al.  
 1180 2008, Occhipinti-Ambrogi et al. 2002, Orel et al. 1987, Poluzzi et al. 1981, Prevedelli et al.  
 1181 2001, Rigotti 2019, Scardi et al. 2000, Seneš 1989, Simonini et al. 2005, Solis-Weiss et al.  
 1182 2001, Targusi 2011, Tomašových et al. 2019, Weber and Zuschin 2013, Zavodnik and  
 1183 Vidakovic 1987, Zucchi Stolfa 1979.

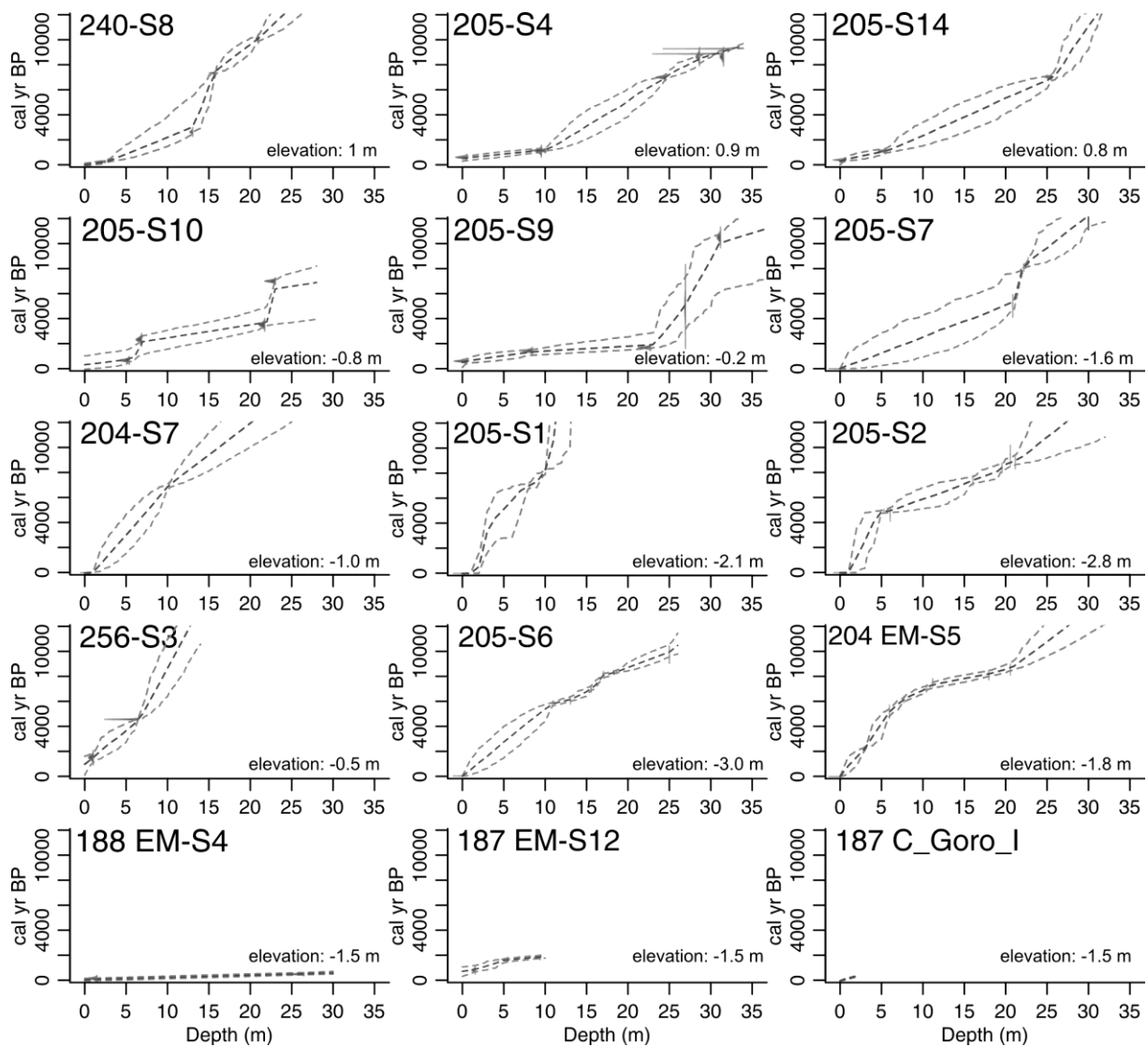
1184

1185

1186

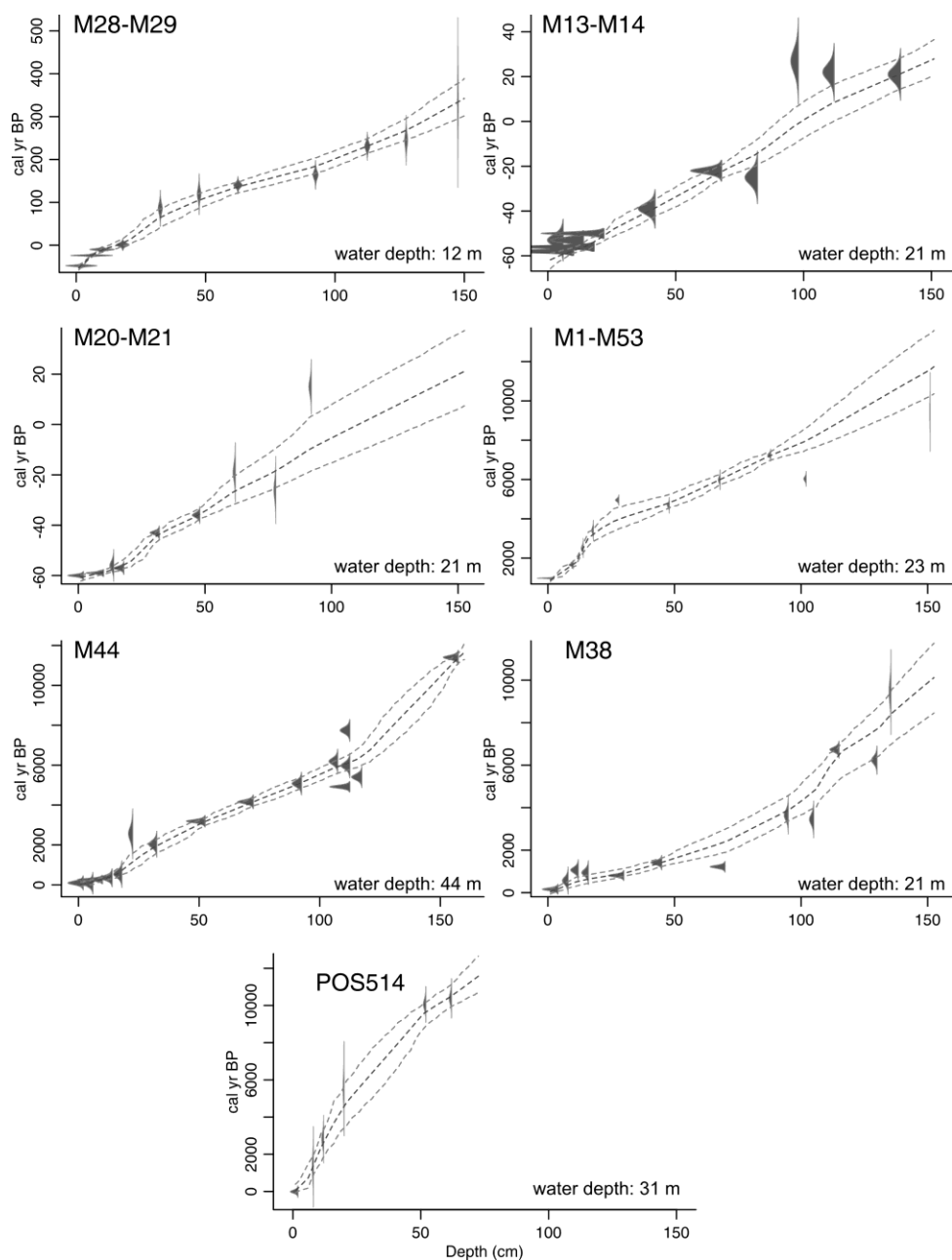
1187

1188



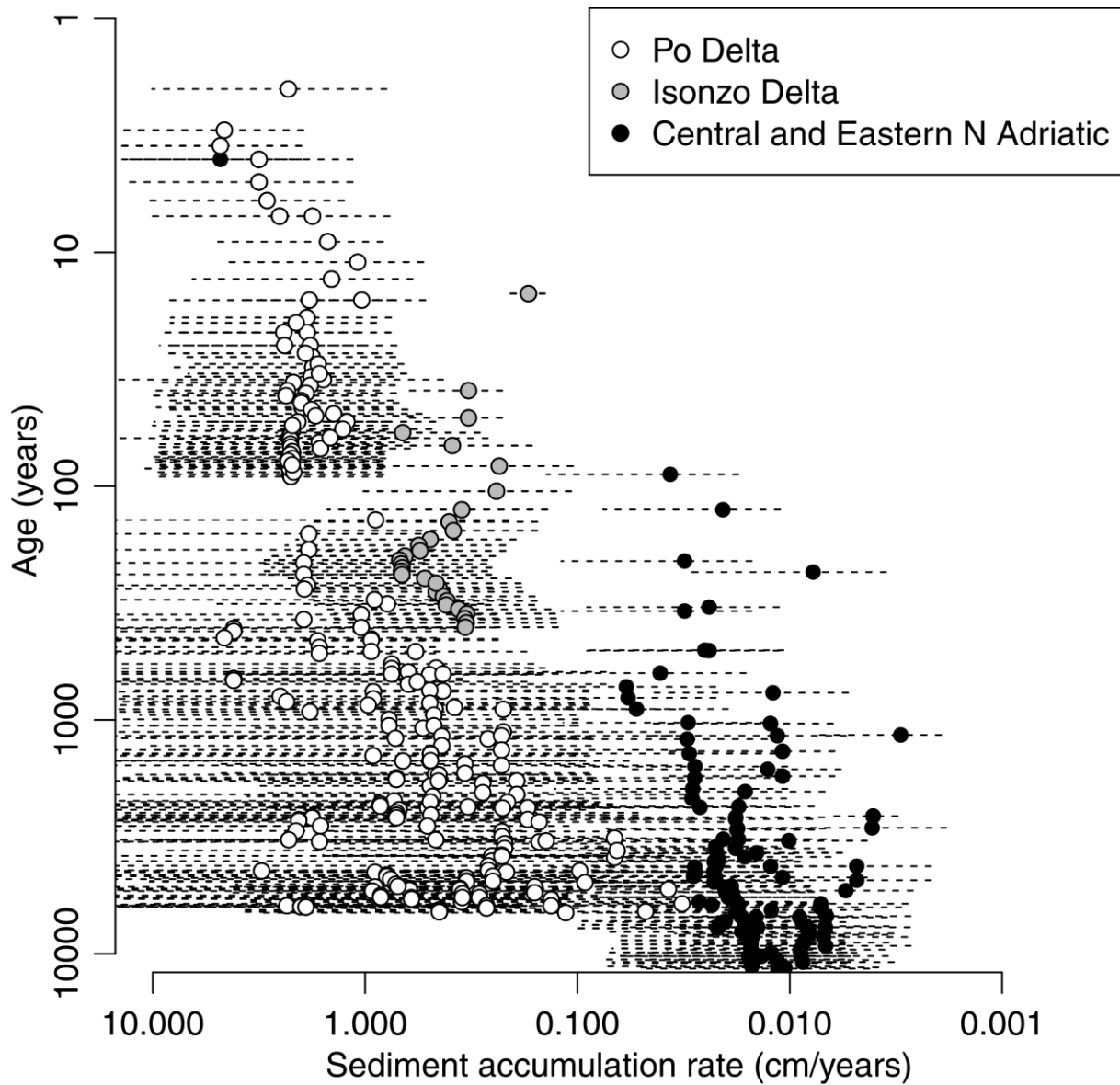
1189

1190 **Figure S2.** Age models for the Po Plain cores. Age model sources: 240-S8 (Campo et al.,  
 1191 2020; Cheli et al., 2021 [sample CE]), 205-S4 (Scarponi et al. 2013; Amorosi et al., 2017;  
 1192 2020; 2021), 205-S14 (Scarponi et al., 2013; Amorosi et al., 2017), 205-S10 (Sarti et al.,  
 1193 2009; Campo et al., 2020), 205-S9 (Sarti et al., 2009; Bruno et al., 2017; Amorosi et al.,  
 1194 2020), 205-S7 (Cibin et al., 2005; Scarponi et al., 2013; Amorosi et al., 2017), 204-S7  
 1195 (Calabrese et al., 2009; Amorosi et al., 2017; Bruno et al., 2019), 205-S1 (Amorosi et al.,  
 1196 2003; Sarti et al., 2009), 205-S2 (Campo et al., 2020; Amorosi et al., 2021), 256-S3 (Severi et  
 1197 al., 2005; Campo et al., 2020), 205-S6 (Sarti et al., 2009; Amorosi et al., 2017, 2020), 204-  
 1198 EM-S5 (Amorosi et al., 2017), 204-EM-S4 (Amorosi et al., 2017), 188-EM-S5 (Amorosi et  
 1199 al., 2017), 187-EM-S12 (Amorosi et al., 2017), 187-C\_Goro\_I (Sarti et al., 2009).



1200

1201 **Figure S3.** Age models for the 1.5 m-long cores, with boxplots representing frequency  
 1202 distributions of geochronological ages (i.e., postmortem ages) of molluscan remains based on  
 1203 amino acid racemization calibrated by  $^{14}\text{C}$ . The age models are partly informed by age  
 1204 distributions but also by additional sedimentological and geochronological data ( $^{210}\text{Pb}$  and  
 1205  $^{14}\text{C}$  of plant remains). Sources for age distributions and age models: Po 3 M13 and Po 4 M21  
 1206 (Tomašových et al. 2018), Panzano M28 (Tomašových et al. 2018), Piran 1 M1 and Piran 2  
 1207 M53 (Mautner et al. 2018, Tomašových et al. 2019), Venice M38 (Gallmetzer et al. 2019),  
 1208 Brijuni M44 (Schnedl et al. 2018, Tomašových et al. 2022), and Poseidon core POS514 –  
 1209 GC-25-5 (Berensmeier et al. 2023).

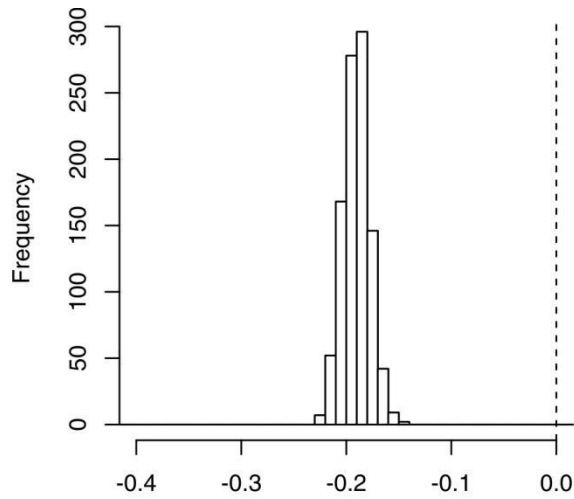


1210

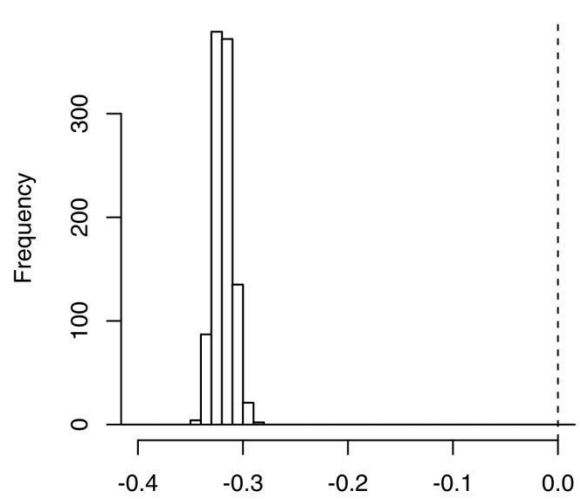
1211

1212 **Figure S4.** The distribution of sediment accumulation rates with respect to assemblage age.  
 1213 Variability in sediment accumulation rates is given by the extent of error bars corresponding  
 1214 to the interquartile range bracketed by the 25<sup>th</sup> and 75<sup>th</sup> percentiles (based on the posterior  
 1215 distribution of sediment accumulation rates).

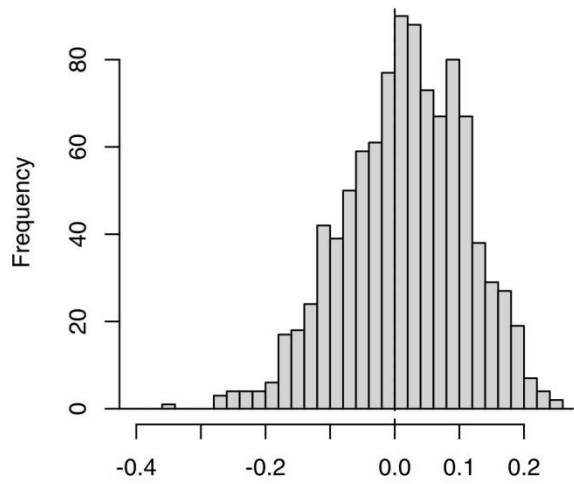
1216



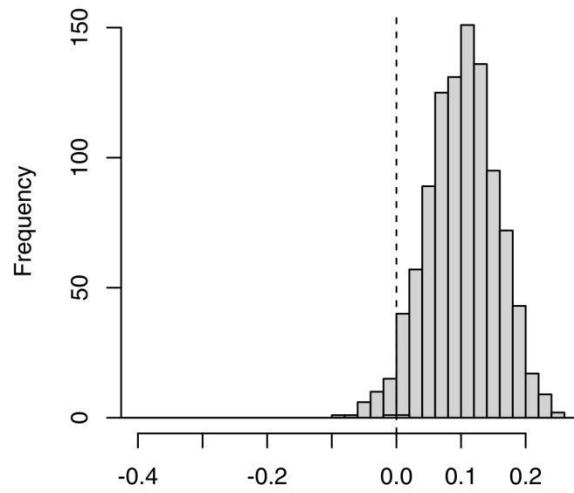
Effect of sedimentation on abundance|depth



Effect of sedimentation on diversity|depth



Effect of abundance on diversity|sedimentation

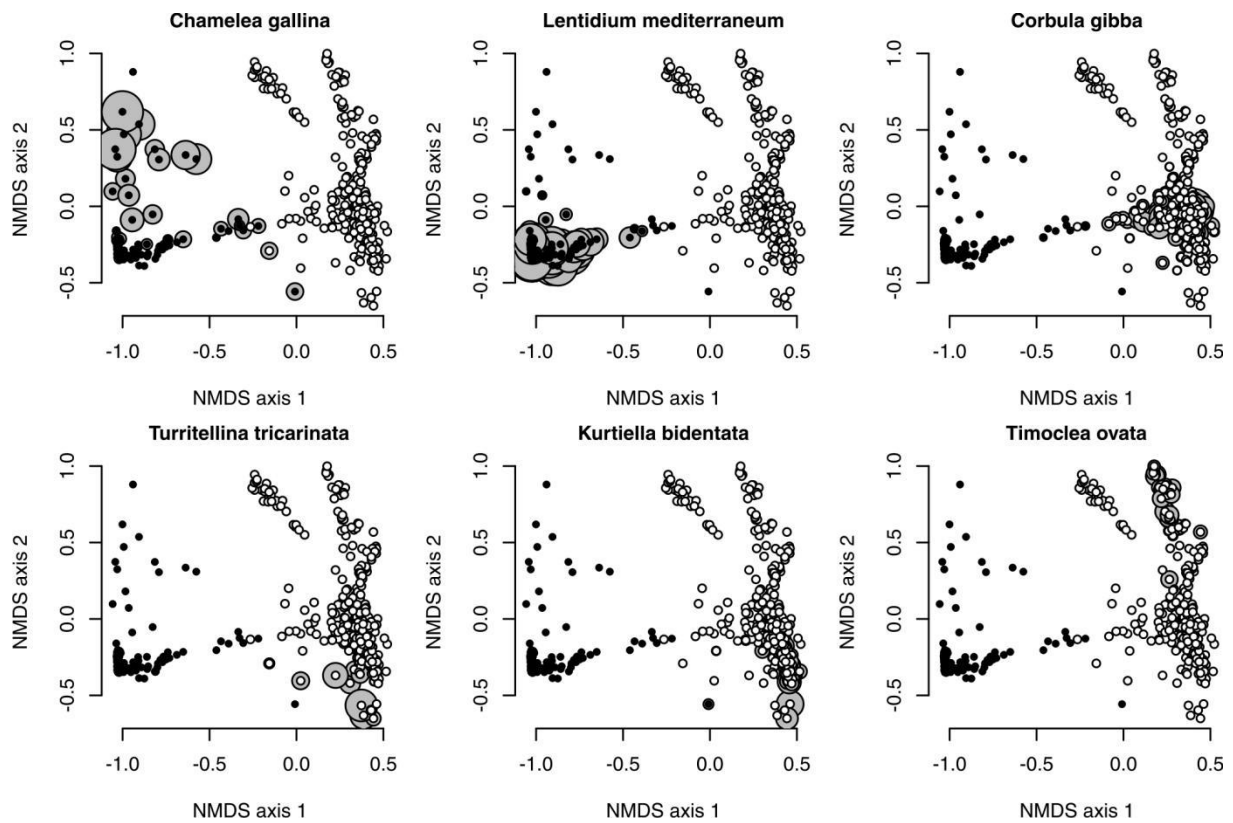


Effect of abundance on diversity|sedimentation+depth

1217

1218

1219 **Figure S5.** The frequency distributions of the fixed effects (effects of sedimentation on  
 1220 abundance and diversity in the upper row and the effect of abundance on diversity  
 1221 conditioned by sedimentation or by both sedimentation and water depth in the bottom row)  
 1222 expected under the repeated sampling of sediment accumulation rates from posterior  
 1223 distributions derived from Bayesian age-depth models. They show that the effects of sediment  
 1224 accumulation are consistently negative and the abundance effect on diversity conditioned by  
 1225 sediment accumulation does not differ from zero.



1226

1227

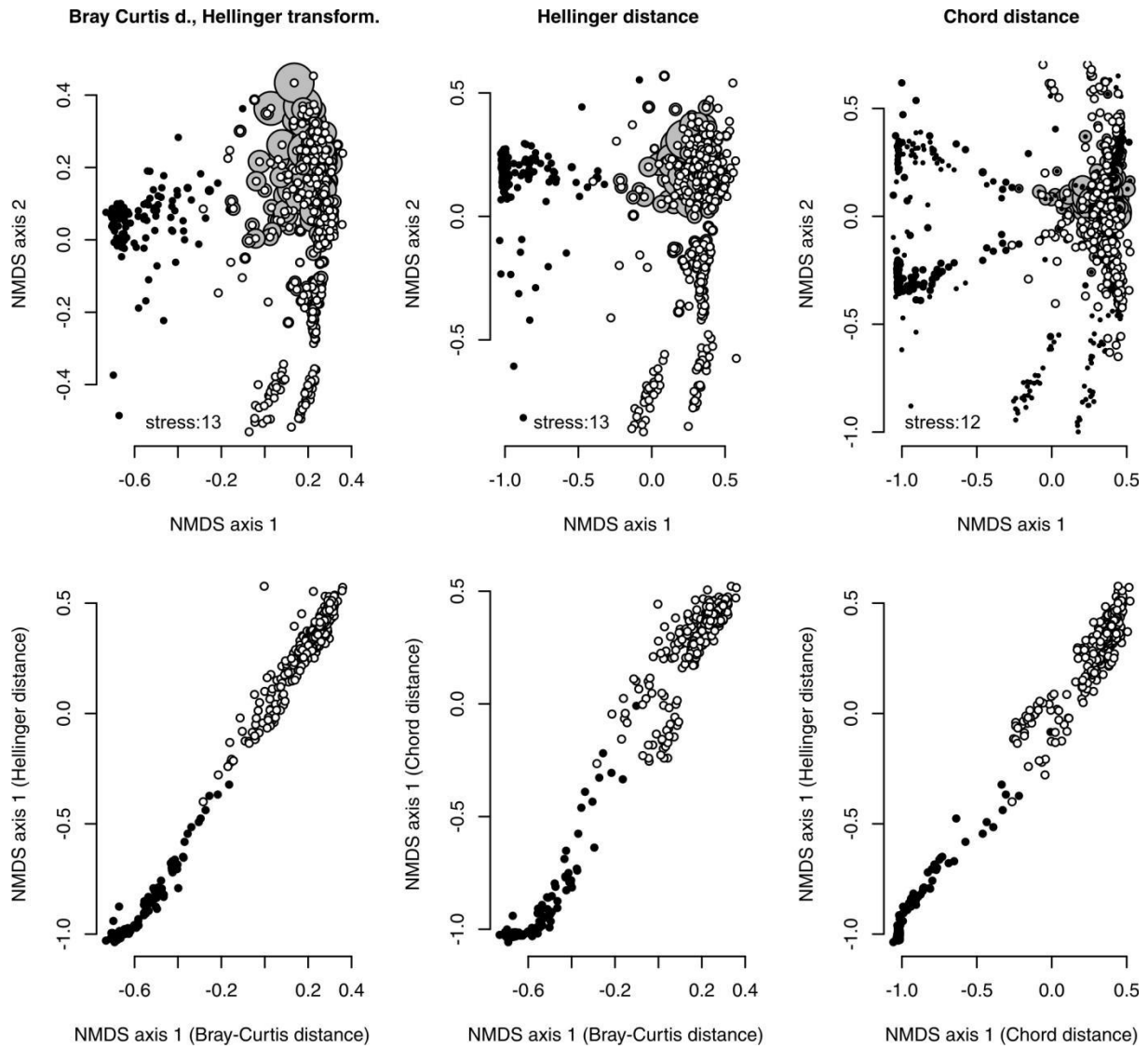
1228 **Figure S6.** NMDS orders fossil molluscan assemblages along a bathymetric gradient, with  
 1229 onshore assemblages possessing negative NMDS axis 1 scores (black circles) and offshore  
 1230 transition and offshore assemblages possessing positive NMDS axis 1 scores (white circles).  
 1231 NMDS is based on proportional abundances and Chord distance. The categorization of  
 1232 assemblages into onshore and offshore groups follows the clusters in Figure S8. The sizes of  
 1233 gray circles are scaled according to the proportional abundances of individual species.

1234

1235

1236

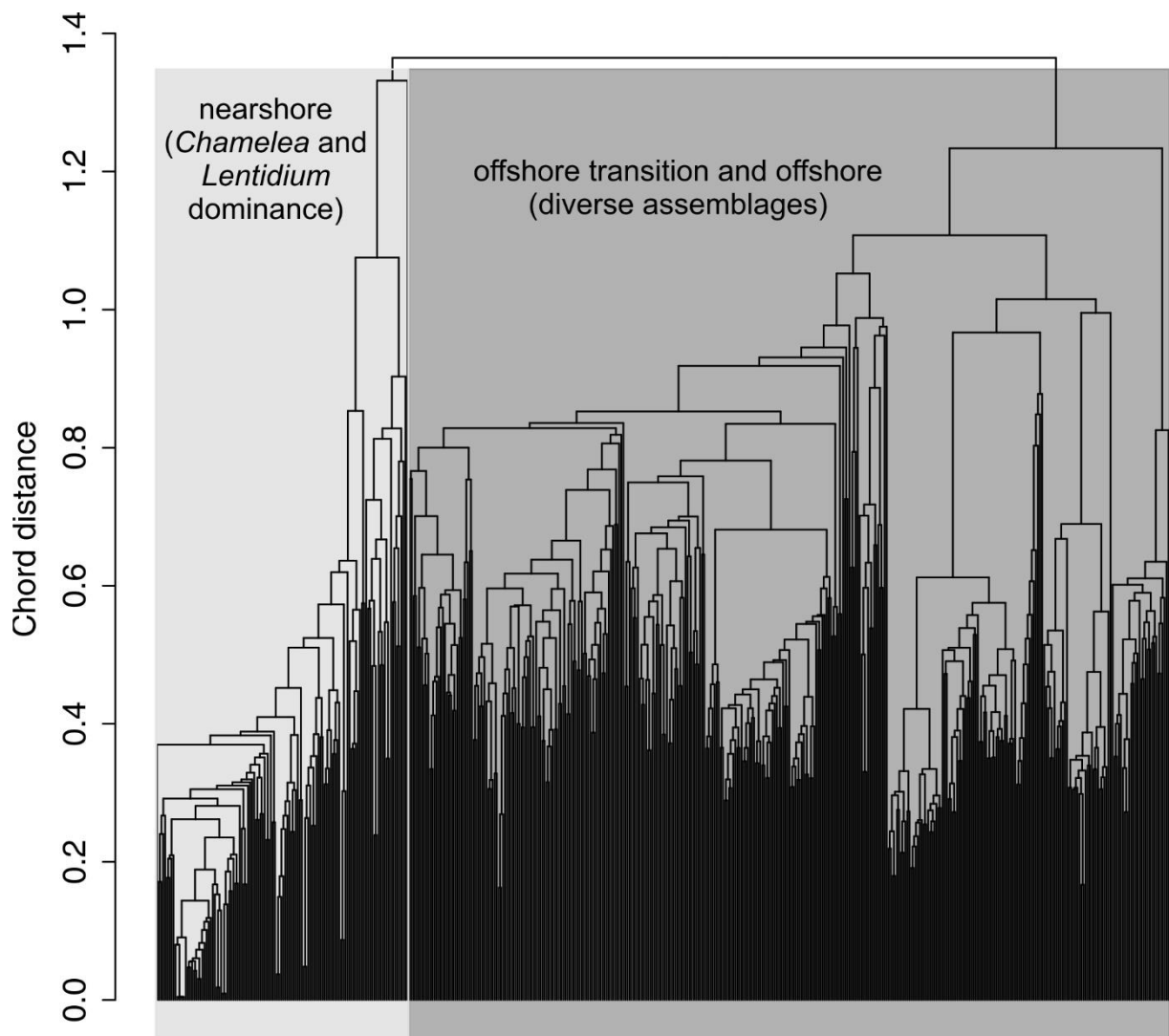




1237

1238 **Figure S7.** Sensitivity of ordinations to the underlying dissimilarity metric. The first NMDS  
 1239 axis is an indicator of water depth the ordering of assemblages is highly similar on the basis of  
 1240 Bray-Curtis, Hellinger and Chord distances. Onshore assemblages are represented by black  
 1241 circles and offshore assemblages by white circles. The categorization of assemblages into  
 1242 these two groups follows the clusters in Figure S8.

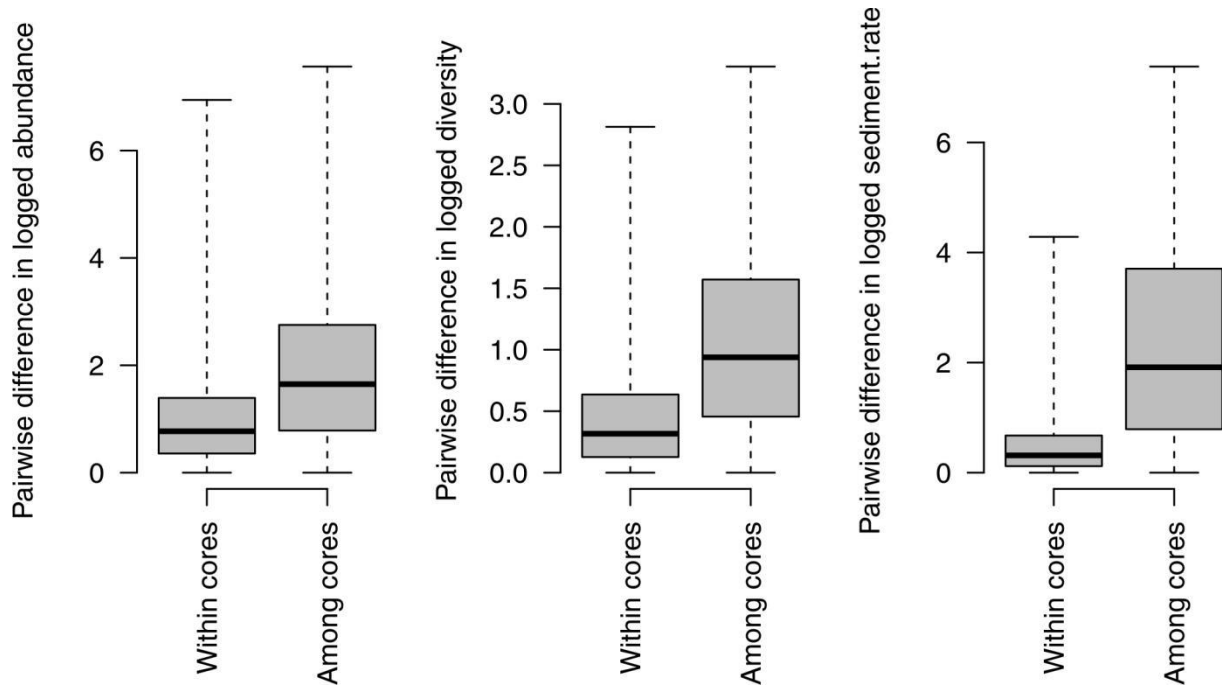
1243



1244

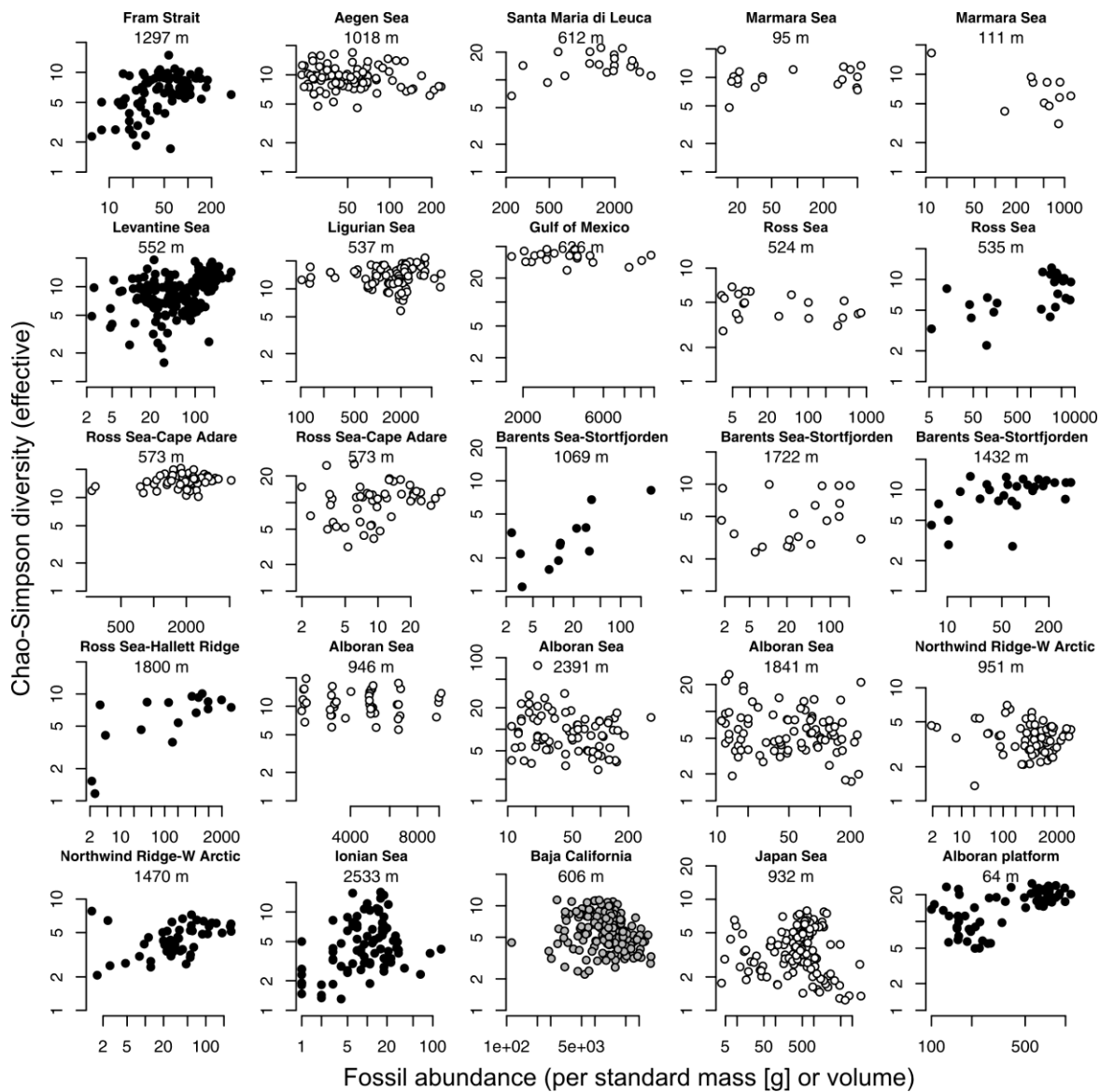
1245 **Figure S8** – Cluster analysis based on average linking method and Chord distance, separating  
 1246 two main groups of assemblages, corresponding to two main environments.

1247



1248

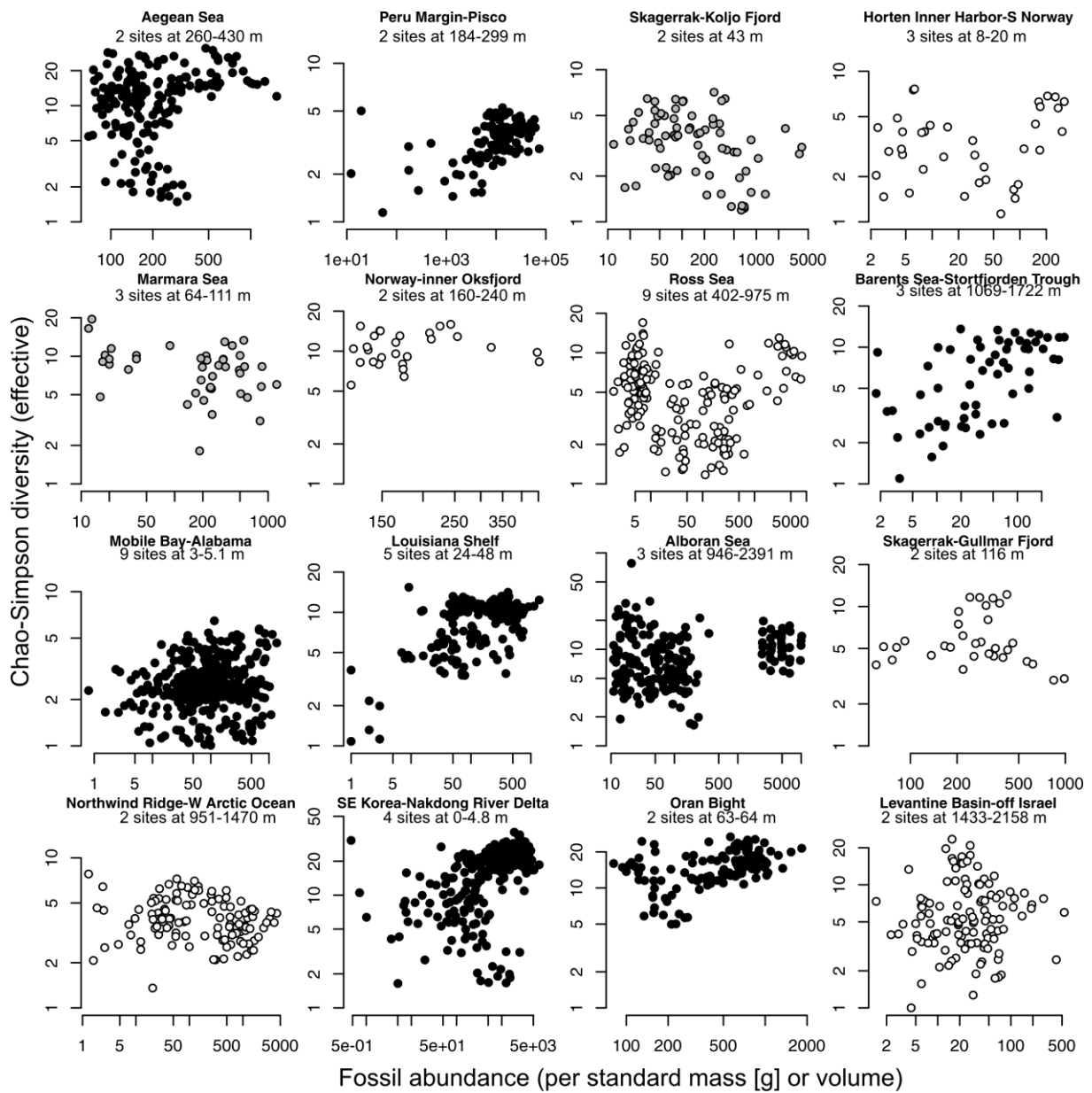
1249 **Figure S9.** Variability in abundance, in diversity, and especially in sediment accumulation is  
 1250 markedly smaller within cores than among cores. Although some subset of cores from the Po  
 1251 coastal plain archive depositional conditions varying in sediment accumulation, the majority  
 1252 of cores in offshore environments were consistently deposited under low sediment  
 1253 accumulation.



1254

1255

1256 **Figure S10.** Local-scale (single-core) abundance-diversity relation in a selection of 25  
 1257 microfossil datasets with benthic foraminifers, with mean sediment accumulation < 0.2 cm/y,  
 1258 coefficient variation in residence time > 0.25, coefficient variation in fossil abundance > 0.5,  
 1259 and gamma-level PIE-based diversity exceeding five species. 12 datasets show a significantly  
 1260 positive relation (black), one dataset shows a significantly negative relation (gray), and 12  
 1261 datasets show insignificant relation (white). Data sources: Table S4.



1262

1263 **Figure S11.** Regional-scale abundance-diversity relation in 16 microfossil datasets (at least  
 1264 two sites per region) with benthic foraminifers. 8 datasets show a significantly positive  
 1265 relation (black), six datasets show a significantly negative relation (gray), and two datasets  
 1266 show insignificant relation (white). Sources: Table S4.

1267 **Supporting tables**

1268 **Table S1** – Diversity and abundance of living (non-averaged) molluscan assemblages in the  
1269 northern Adriatic Sea, with source references. Data columns correspond to the reference,  
1270 dataset ID (optional), latitude, longitude and water depth (m) of the assemblage, raw sample  
1271 size and total abundance/m<sup>2</sup>. Diversity indices correspond to the effective number of species  
1272 based on the PIE-based and Simpson index, the effective number of species based on the  
1273 Shannon index, and evenness values based on the Pielou J and Bulla O.

1274 **Table S2** – Diversity and abundance of fossil (time-averaged) molluscan assemblages  
1275 collected in sediment cores in the northern Adriatic Sea. Individual fossil assemblages are in  
1276 rows, data columns correspond to the core ID, sediment depth (cm), increment thickness (cm),  
1277 systems tract (HST – highstand systems tract, MFZ – maximum flooding zone, TST –  
1278 transgressive systems tract), facies association/environment, sediment accumulation (cm/y),  
1279 sample size, fossil abundance/dm<sup>3</sup>, Shannon H, Gini-Simpson index, Probability of  
1280 interspecific encounter, the effective number of species (Simpson and PIE), evenness values  
1281 based on the Pielou J and Bulla O, and the location of the assemblages along the first NMDS  
1282 axis.

1283 **Table S3** - Abundance-diversity relations in 30 geographic datasets with benthic foraminiferal  
1284 living assemblages (LADR), with references.

1285 **Table S4** – Abundance-diversity relations in 73 benthic foraminiferal fossil assemblages  
1286 (FADR) in local stratigraphic series and in regional datasets, with references.

1287 **Table S5** – Input chronological data for Bacon function.

1288

1289 **Supporting scripts**

1290 R language scripts for models and species-time relation

1291 R language scripts for cartoons and data analyses

1292

1293 **Supporting references – methods, age data, molluscan fossil assemblages**

1294 Amorosi, A., Centineo, M. C., Colalongo, M. L., Pasini, G., Sarti, G., and Vaiani, S.C. 2003.

1295 Facies architecture and latest Pleistocene–Holocene depositional history of the Po Delta

- 1296 (Comacchio area), Italy. *Journal of Geology* 111, 39-56.
- 1297 Amorosi, A., Bruno, L., Campo, B., Morelli, A., Rossi, V., Scarponi, D., Hong, W., Bohacs,  
1298 K.M. and Drexler, T.M., 2017. Global sea-level control on local parasequence architecture  
1299 from the Holocene record of the Po Plain, Italy. *Marine and Petroleum Geology* 87, 99-111.
- 1300 Amorosi, A., Bruno, L., Campo, B., Costagli, B., Dinelli, E., Hong, W., Sammartino, I. and  
1301 Vaiani, S.C., 2020. Tracing clinothem geometry and sediment pathways in the prograding  
1302 Holocene Po Delta system through integrated core stratigraphy. *Basin Research* 32, 206-215.
- 1303 Amorosi A., Bruno L., Campo B., Costagli B., Hong W., Picotti V., Vaiani S.C., 2021.  
1304 Deformation patterns of upper Quaternary strata and their relation to active tectonics, Po  
1305 Basin, Italy. *Sedimentology* 68, 402-424.
- 1306 Berensmeier, M., Tomašových, A., Nawrot, R., Cassin, D., Zonta, R., Koubová, I. and  
1307 Zuschin, M., 2023. Stratigraphic expression of the human impacts in condensed deposits of  
1308 the Northern Adriatic Sea. *Geological Society, London, Special Publications* 529, 195-222.
- 1309 Blaauw, M., Christen, J.A., Lopez, M.A.A., Vazquez, J.E., Belding, T., Theiler, J., Gough, B.,  
1310 Karney, C., Rcpp, L. and Blaauw, M.M., 2021. Package 'rbacon'. Age-depth modelling using  
1311 Bayesian statistics. Version: 3.1.1. <https://CRAN.R-project.org/package=rbacon>
- 1312 Blaauw, M. and Christen, J.A., 2011. Flexible paleoclimate age-depth models using an  
1313 autoregressive gamma process. *Bayesian Analysis* 6:457-474.
- 1314 Bruno L., Bohacs K.M., Campo B., Drexler T.M., Rossi V., Sammartino I., Scarponi D.,  
1315 Hong, W., and Amorosi A. 2017. Early Holocene transgressive palaeogeography in the Po  
1316 coastal plain (northern Italy). *Sedimentology* 64, 1792 - 1816
- 1317 Bruno, L., Campo, B., Di Martino, A., Hong, W. and Amorosi, A. 2019. Peat layer  
1318 accumulation and post-burial deformation during the mid-late Holocene in the Po coastal  
1319 plain (Northern Italy). *Basin Research* 31, 621-639.
- 1320 Calabrese L., Centineo M.C., Cibin U., Di Cocco I., 2009. Note Illustrative della Carta  
1321 Geologica alla scala 1:50.000: Portomaggiore. *Servizio geologico sismico e dei suoli -*  
1322 *Regione Emilia Romagna*, 98 pp.
- 1323 Campo B., Bruno L., Amorosi A., 2020. Basin-scale stratigraphic correlation of late  
1324 Pleistocene-Holocene (MIS 5e-MIS 1) strata across the rapidly subsiding Po Basin (northern

1325 Italy). *Quaternary Science Reviews* 237, 106300.

1326 Cheli A, Mancuso A, Azzarone M, Fermani S, Kaandorp J, Marin F, et al. 2021. Climate  
1327 variation during the Holocene influenced the skeletal properties of *Chamelea gallina* shells in  
1328 the North Adriatic Sea (Italy). *PLoS ONE* 16, e0247590.

1329 Cibir U. et al., 2005 Note illustrative della Carta geologica d'Italia alla scala 1:50.00: Forlì-  
1330 Cervia. *Servizio geologico sismico e dei suoli - Regione Emilia Romagna*, 104 pp.

1331 Gallmetzer, I., Haselmair, A., Tomašových, A., Stachowitsch, M. and Zuschin, M., 2017.  
1332 Responses of molluscan communities to centuries of human impact in the northern Adriatic  
1333 Sea. *Plos One* 12, e0180820.

1334 Gallmetzer, I., Haselmair, A., Tomašových, A., Mautner, A.K., Schnedl, S.M., Cassin, D.,  
1335 Zonta, R. and Zuschin, M., 2019. Tracing origin and collapse of Holocene benthic baseline  
1336 communities in the northern Adriatic Sea. *Palaios* 34, 121-145.

1337 Gouhier T.C. and Guichard F. 2014. Synchrony: quantifying variability in space and  
1338 time. *Methods in Ecology and Evolution*, 5, 524–533. R package version  
1339 0.3.8, <http://synchrony.r-forge.r-project.org>.

1340 Haselmair, A., Gallmetzer, I., Tomašových, A., Wieser, A.M., Übelhör, A. and Zuschin, M.,  
1341 2021. Basin-wide infaunalisation of benthic soft-bottom communities driven by  
1342 anthropogenic habitat degradation in the northern Adriatic Sea. *Marine Ecology Progress*  
1343 *Series* 671, 45-65.

1344 Hsieh, T.C., Ma, K.H. and Chao, A., 2016. iNEXT: an R package for rarefaction and  
1345 extrapolation of species diversity (Hill numbers). *Methods in Ecology and Evolution*, 7,  
1346 1451-1456.

1347 Hubbell, S.P., 2001. The unified neutral theory of biodiversity and biogeography. *Princeton:*  
1348 *Princeton University Press*.

1349 Kidwell, S.M., 2002. Time-averaged molluscan death assemblages: palimpsests of richness,  
1350 snapshots of abundance. *Geology*, 30, 803-806.

1351 Lefcheck J.S. 2016. piecewiseSEM: Piecewise structural equation modeling in R for ecology,  
1352 evolution, and systematics. *Methods in Ecology and Evolution*, 7, 573-579.

1353 Mautner, A.K., Gallmetzer, I., Haselmair, A., Schnedl, S.M., Tomašových, A. and Zuschin,



1354 M., 2018. Holocene ecosystem shifts and human-induced loss of *Arca* and *Ostrea* shell beds  
1355 in the north-eastern Adriatic Sea. *Marine Pollution Bulletin* 126, 19-30.

1356 Mazerolle M.J. 2023. AICcmodavg: Model selection and multimodel inference based on  
1357 (Q)AIC(c). R package version 2.3.3, <https://cran.r-project.org/package=AICcmodavg>.

1358 Mersmann, O., Trautmann, H., Steuer, D., and Bornkamp, B. 2018. truncnorm: Truncated  
1359 Normal Distribution. Package 'truncnorm'. *R package version* 1.0-9. R ( $\geq 3.4.0$ ),  
1360 <https://github.com/olafmersmann/truncnorm>

1361 Oksanen J., Blanchet G.F., Friendly M., Kindt R., Legendre P., McGlenn D., Minchin P.R.,  
1362 O'Hara B., Simpson G.L., Solymos P., Stevens M.H.H., Szoecs E. and Wagner H. 2020.  
1363 vegan: Community Ecology Package. R package version 2.5-7. [https://CRAN.R-](https://CRAN.R-project.org/package=vegan)  
1364 [project.org/package=vegan](https://CRAN.R-project.org/package=vegan)

1365 Patil I., Makowski D., Ben-Shachar M., Wiernik B., Bacher E., and Lüdecke D. 2022.  
1366 datawizard: An R Package for Easy Data Preparation and Statistical Transformations. *Journal*  
1367 *of Open Source Software*, **7**, 4684. doi:10.21105/joss.04684.

1368 Pinheiro J., Bates D., R Core Team 2023. *nlme: Linear and Nonlinear Mixed Effects Models*.  
1369 R package version 3.1-164, <https://CRAN.R-project.org/package=nlme>.

1370 Sarti G. et al., 2009 Note illustrative della Carta geologica d'Italia alla scala 1:50.00:  
1371 Comacchio. Servizio geologico sismico e dei suoli - Regione Emilia Romagna, 126 pp.

1372 Scarponi, D. and Kowalewski, M., 2004. Stratigraphic paleoecology: bathymetric signatures  
1373 and sequence overprint of mollusk associations from upper Quaternary sequences of the Po  
1374 Plain, Italy. *Geology*, **32**, 989-992.

1375 Scarponi, D. and Kowalewski M. 2007. Sequence stratigraphic anatomy of diversity patterns:  
1376 Late Quaternary benthic mollusks of the Po Plain, Italy. *Palaios*, **22**, 296-305.

1377 Scarponi, D., Kaufman, D., Amorosi, A. and Kowalewski, M., 2013. Sequence stratigraphy  
1378 and the resolution of the fossil record. *Geology* **41**, 239-242.

1379 Schnedl, S.M., Haselmair, A., Gallmetzer, I., Mautner, A.K., Tomašových, A. and Zuschin,  
1380 M., 2018. Molluscan benthic communities at Brijuni Islands (northern Adriatic Sea) shaped  
1381 by Holocene sea-level rise and recent human eutrophication and pollution. *Holocene* **28**,  
1382 1801-1817.

- 1383 Schumacker R.E., Lomax R.G. 2010. A beginner's guide to structural equation modelling.  
1384 Routledge Taylor and Francis Group, 3<sup>rd</sup> Edition.
- 1385 Severi et al., 2005. Note illustrative della Carta geologica d'Italia alla scala 1:50.000: Rimini.  
1386 *Servizio geologico sismico e dei suoli - Regione Emilia Romagna*, 143 pp.
- 1387 Tomašových, A., Gallmetzer, I., Haselmair, A., Kaufman, D.S., Vidović, J. and Zuschin, M.,  
1388 2017. Stratigraphic unmixing reveals repeated hypoxia events over the past 500 yr in the  
1389 northern Adriatic Sea. *Geology* 45, 363-366.
- 1390 Tomašových, A., Gallmetzer, I., Haselmair, A., Kaufman, D.S., Kralj, M., Cassin, D., Zonta,  
1391 R. and Zuschin, M., 2018. Tracing the effects of eutrophication on molluscan communities in  
1392 sediment cores: outbreaks of an opportunistic species coincide with reduced bioturbation and  
1393 high frequency of hypoxia in the Adriatic Sea. *Paleobiology* 44, 575-602.
- 1394 Tomašových, A., Gallmetzer, I., Haselmair, A., Kaufman, D.S., Mavrič, B. and Zuschin, M.,  
1395 2019. A decline in molluscan carbonate production driven by the loss of vegetated habitats  
1396 encoded in the Holocene sedimentary record of the Gulf of Trieste. *Sedimentology* 66, 781-  
1397 807.
- 1398 Tomašových, A., Gallmetzer, I., Haselmair, A. and Zuschin, M., 2022. Inferring time  
1399 averaging and hiatus durations in the stratigraphic record of high-frequency depositional  
1400 sequences. *Sedimentology* 69, 1083-1118.
- 1401 Wickham H. 2016. *ggplot2: Elegant Graphics for Data Analysis*. Springer-Verlag New York.  
1402 ISBN 978-3-319-24277-4, <https://ggplot2.tidyverse.org>.
- 1403 Wickham H., François R., Henry L., Müller K., and Vaughan D. 2023. *dplyr: A Grammar of*  
1404 *Data Manipulation*. R package version 1.1.4,  
1405 <https://github.com/tidyverse/dplyr>, <https://dplyr.tidyverse.org>.
- 1406 Wood S.N. 2011. Fast stable restricted maximum likelihood and marginal likelihood  
1407 estimation of semiparametric generalized linear models. *Journal of the Royal Statistical*  
1408 *Society B*, **73**, 3-36.
- 1409
- 1410 **Supporting references – living molluscan assemblages**

1411 Ambrogi, R. and Ambrogi, A.O., 1985. The estimation of secondary production of the marine  
1412 bivalve *Spisula subtruncata* (da Costa) in the area of the Po River delta. *Marine Ecology* 6,  
1413 239-250.

1414 Ambrogi, R., Colangelo, M.A., Fontana, P., Gatto, M., Sei, S. and Tracanella, E., 1995. La  
1415 demografia del bivalve *Lentidium mediterraneum* nella zona di mare antistante il delta del Po.  
1416 *Atti 6 congresso Società Italiana di Ecologia* 16, 165-167.

1417 ARPAE 2010-2019. Valutazione dello stato delle acque marine costiere. Monitoraggio delle  
1418 acque marino costiere e classificazione dello stato di qualità. *Regione Agenzia Prevenzione*  
1419 *Ambiente Energia Emilia-Romagna*. [https://www.arpae.it/it/temi-ambientali/mare/report-e-](https://www.arpae.it/it/temi-ambientali/mare/report-e-bollettini/stato-acque-marine)  
1420 [bollettini/stato-acque-marine](https://www.arpae.it/it/temi-ambientali/mare/report-e-bollettini/stato-acque-marine)  
1421 <https://www.arpae.it/it/temi-ambientali/mare/report-e-bollettini/stato-acque-marine>

1422 Chiantore, M., Bedulli, D., Cattaneo-Vietti, R., Schiaparelli, S. and Albertelli, G., 2001.  
1423 Long-term changes in the Mollusc-Echinoderm assemblages in the north and coastal middle  
1424 Adriatic Sea. *Atti della Associazione Italiana di Oceanologia e Limnologia*, 14, 63-75.

1425 ENEA. *Italian Mollusc Census Database of the Italian National Agency for New*  
1426 *Technologies, Energy and Sustainable Economic Development*.  
1427 <http://www.santateresa.enea.it/wwwste/malaco/home.htm>.

1428 Forni, G. and Ambrogi, A.O., 2005. Struttura di popolazione del bivalve *Lentidium*  
1429 *mediterraneum* e variazioni ambientali in Nord Adriatico. *Biologia Marina Mediterranea* 12,  
1430 277-280.

1431 ISPRA (2012) Studio delle comunita' bentoniche. Monitoraggio del Terminale GNL – area  
1432 della condotta offshore – Fase di esercizio provvisorio (2 E). *Istituto Superiore per la*  
1433 *Protezione e la Ricerca Ambientale*.

1434 Mavrič, B., Orlando-Bonaca, M., Bettoso, N. and Lipej, L., 2010. Soft-bottom  
1435 macrozoobenthos of the southern part of the Gulf of Trieste: faunistic, biocoenotic and  
1436 ecological survey. *Acta Adriatica* 51, 203-216.

1437 Moodley, L., Heip, C.H. and Middelburg, J.J., 1998. Benthic activity in sediments of the  
1438 northwestern Adriatic Sea: sediment oxygen consumption, macro-and meiofauna  
1439 dynamics. *Journal of Sea Research* 40, 263-280.

1440 N'Siala, G. M., V. Grandi, M. Iotti, G. Montanari, D. Prevedelli, and R. Simonini. 2008.  
1441 Responses of a northern Adriatic Ampelisca–Corbula community to seasonality and short-  
1442 term hydrological changes in the Po River. *Marine Environmental Research* 66, 466–476

1443 Occhipinti-Ambrogi, A., Favruzzo, M. and Savini, D., 2002. Multi-annual variations of  
1444 macrobenthos along the Emilia-Romagna Coast (Northern Adriatic). *Marine Ecology*, 23,  
1445 307-319.

1446 Orel, G., Marocco, R., Vio, E., Del Piero, D. and Della Seta, G., 1987. Sedimenti e biocenosi  
1447 bentoniche tra la foce del Po ed il Golfo di Trieste (Alto Adriatico). *Bulletin d'Ecologie*, 18,  
1448 229-241.

1449 Prevedelli, D., Simonini, R. and Ansaloni, I., 2001. Relationship of non-specific  
1450 commensalism in the colonisation of the deep layers of sediment. *Journal of the Marine*  
1451 *Biological Association of the United Kingdom* 81, 897-901.

1452 Pitacco, V., Mistri, M., Aleffi, I.F., Lardicci, C., Prato, S., Tagliapietra, D. and Munari, C.,  
1453 2019. Spatial patterns of macrobenthic alpha and beta diversity at different scales in Italian  
1454 transitional waters (central Mediterranean). *Estuarine, Coastal and Shelf Science*, 222, 126-  
1455 138.

1456 Poluzzi, A., Sabelli, B. and Taviani, M., 1981. Auto-sinecologia dei Molluschi: dei fondi  
1457 mobili del delta settentrionale del Po (Estate 1980). *Bollettino della Societa Paleontologica*  
1458 *Italiana*, 21, 169-178.

1459 Rigotii, L. 2019. Studio e caratterizzazione preliminari di sedimento e macrozoobenthos in  
1460 due stazioni marine costiere in località Ca' Roman (VE). *Dipartimento di Biologia*,  
1461 *Universita' degli studi di Padova, Master thesis*.

1462 Scardi, M., R. Crema, P. Di Dato, E. Fresi, and G. Orel. 2000. Le comunità bentoniche  
1463 dell'Alto Adriatico: un'analisi preliminare dei cambiamenti strutturali dagli anni'30 ad oggi.  
1464 Pp. 95–108 in O. Giovanardi, ed. Impact of trawl fishing on benthic communities. *Istituto*  
1465 *Centrale per la Ricerca Scientifica e Tecnologica Applicata al Mare, Rome*.

1466 Seneš, J., 1989. North Adriatic inter-island shelf ecosystems of the Rovinj area. *Geologica*  
1467 *Carpathica* 40, 333-354.

- 1468 Simonini, R., I. Ansaloni, A. B. Pagliai, and D. Prevedelli. 2004. Organic enrichment and  
1469 structure of the macrozoobenthic community in the northern Adriatic Sea in an area facing  
1470 Adige and Po mouths. *ICES Journal of Marine Science* 61, 871–881.
- 1471 Solis-Weiss, V., Rossin, P., Aleffi, F., Bettoso, N., Orel, G., Vrišer, B., 2001. Gulf of Trieste:  
1472 sensitivity areas using benthos and GIS techniques. In: Özhan, E. (Ed.), *Proceedings of the*  
1473 *Fifth International Conference on the Mediterranean Coastal Environment*. Ankara, Turkey,  
1474 1567–1578. [http://ipt.vliz.be/eurobis/resource?r=macroben\\_lbmrev\\_evco](http://ipt.vliz.be/eurobis/resource?r=macroben_lbmrev_evco)
- 1475 Targusi, M. 2011. I crostacei Anfipodi quali descrittori delle comunità bentoniche di ambienti  
1476 marino costieri interessati da attività antropiche. *Universita degli studi di Napoli Federico II,*  
1477 *Dissertation thesis*.
- 1478 Weber, K. and Zuschin, M., 2013. Delta-associated molluscan life and death assemblages in  
1479 the northern Adriatic Sea: implications for paleoecology, regional diversity and  
1480 conservation. *Palaeogeography, Palaeoclimatology, Palaeoecology*, 370, 77-91.
- 1481 Zucchi Stolfa M.L. 1979. Lamellibranchi recenti delle lagune di Grado e di Marano.  
1482 *Atti del Museo Friulano di Storia Naturale* 1, 41-60.
- 1483 Zavodnik, D. and Vidakovic, J., 1987. Report on bottom fauna in two Northern Adriatic areas  
1484 presumed to be influenced by inputs. *Report of the FAO/UNEP Meeting on the Effects of*  
1485 *Pollution on Marine Ecosystems, Food and Agriculture Organization of the United Nations,*  
1486 *Fisheries Report*, 352, Supplement, 263-279.
- 1487
- 1488 **Supporting references – living benthic foraminiferal assemblages**
- 1489 Alves Martins, M.V., Hohenegger, J., Frontalini, F., Dias, J.M.A., Geraldès, M.C. and Rocha,  
1490 F., 2019. Dissimilarity between living and dead benthic foraminiferal assemblages in the  
1491 Aveiro Continental Shelf (Portugal). *PLoS One*, 14, e0209066.
- 1492 Avnaim-Katav, S., Almogi-Labin, A., Kanari, M. and Herut, B., 2020. Living benthic  
1493 foraminifera of southeastern Mediterranean ultra-oligotrophic shelf habitats: Implications for  
1494 ecological studies. *Estuarine, Coastal and Shelf Science*, 234, 106633

1495 Barras, C., Jorissen, F.J., Labrune, C., Andral, B. and Boissery, P., 2014. Live benthic  
1496 foraminiferal faunas from the French Mediterranean Coast: Towards a new biotic index of  
1497 environmental quality. *Ecological Indicators*, 36, 719-743.

1498 Dimiza, M.D., Koukousioura, O., Triantaphyllou, M.V. and Dermitzakis, M.D., 2016. Live  
1499 and dead benthic foraminiferal assemblages from coastal environments of the Aegean Sea  
1500 (Greece): Distribution and diversity. *Revue de Micropaléontologie*, 59, 19-32

1501 Dessandier, P.A., Bonnin, J., Kim, J.H. and Racine, C., 2018. Comparison of living and dead  
1502 benthic foraminifera on the Portuguese margin: Understanding the taphonomical processes.  
1503 *Marine Micropaleontology*, 140, 1-16

1504 Diz, P. and Francés, G., 2008. Distribution of live benthic foraminifera in the Ría de Vigo  
1505 (NW Spain). *Marine Micropaleontology*, 66, 165-191

1506 Fentimen, R., Rüggeberg, A., Lim, A., Kateb, A.E., Foubert, A., Wheeler, A.J. and  
1507 Spezzaferri, S., 2018. Benthic foraminifera in a deep-sea high-energy environment: the Moira  
1508 Mounds (Porcupine Seabight, SW of Ireland). *Swiss Journal of Geosciences*, 111 561-572.

1509 Harloff, J. and Mackensen, A., 1997. Recent benthic foraminiferal associations and ecology  
1510 of the Scotia Sea and Argentine Basin. *Marine Micropaleontology*, 31, 1-29.

1511 Jiang, F., Fan, D., Zhao, Q., Wu, Y., Ren, F., Liu, Y. and Li, A., 2023. Comparison of alive  
1512 and dead benthic foraminiferal fauna off the Changjiang Estuary: Understanding water-mass  
1513 properties and taphonomic processes. *Frontiers in Marine Science*, 10, 1114337.

1514 Licari, L. and Mackensen, A., 2005. Benthic foraminifera off West Africa (1° N to 32° S): Do  
1515 live assemblages from the topmost sediment reliably record environmental variability?.  
1516 *Marine Micropaleontology*, 55, 205-233

1517 Lutze, GF (1974): Benthische Foraminiferen in Oberflächen-Sedimenten des Persischen  
1518 Golfes. Teil 1: Arten. *Meteor Forschungsergebnisse, Deutsche Forschungsgemeinschaft,*  
1519 *Reihe C Geologie und Geophysik*, C17, 1-66

1520 Mackensen, A., Fu, D.K., Grobe, H. and Schmiedl, G., 1993. Benthic foraminiferal  
1521 assemblages from the eastern South Atlantic Polar Front region between 35 and 57 S:  
1522 Distribution, ecology and fossilization potential. *Marine Micropaleontology*, 22, 33-69.

1523 Mallon, J., Glock, N., and Schönfeld, J. 2012, The response of benthic foraminifera to low-  
1524 oxygen conditions of the Peruvian oxygen minimum zone. *In: Altenbach, A., Bernhard J.M.*  
1525 *and Seckbach J., eds, Anoxia: Evidence for Eukaryote Survival and Paleontological*  
1526 *Strategies*, Springer, Dordrecht, 305–321.

1527 In: ANOXIA : , ed. by Altenbach, Alexander V., Bernhard, Joan M. and Seckbach, Joseph.  
1528 *Cellular Origin, Life in Extreme Habitats and Astrobiology*, 21

1529 Martins, M.V.A., Hohenegger, J., Frontalini, F., Miranda, P., da Conceição Rodrigues, M.A.  
1530 and Dias, J.M.A., 2016. Comparison between the dead and living benthic foraminiferal  
1531 assemblages in Aveiro Lagoon (Portugal). *Palaeogeography, Palaeoclimatology,*  
1532 *Palaeoecology*, 455, 16-32.

1533 Martins, M.V.A., Hohenegger, J., Martínez-Colón, M., Frontalini, F., Bergamashi, S., Laut,  
1534 L., Belart, P., Mahiques, M., Pereira, E., Rodrigues, R. and Terroso, D., 2020. Ecological  
1535 quality status of the NE sector of the Guanabara Bay (Brazil): A case of living benthic  
1536 foraminiferal resilience. *Marine Pollution Bulletin*, 158, 111449

1537 Melis, R. and Violanti, D., 2006. Foraminiferal biodiversity and Holocene evolution of the  
1538 Phetchaburi coastal area (Thailand Gulf). *Marine Micropaleontology*, 61, 94-115.

1539 Mojtahid, M., Jorissen, F., Lansard, B., Fontanier, C., Bombled, B. and Rabouille, C., 2009.  
1540 Spatial distribution of live benthic foraminifera in the Rhône prodelta: Faunal response to a  
1541 continental–marine organic matter gradient. *Marine Micropaleontology*, 70, 177-200

1542 Oron, S., Friedlander, A.M., Sala, E. and Goodman-Tchernov, B.N., 2022. Recent shallow  
1543 water foraminifera from the Selvagens Islands (Northeast Atlantic)–Assemblage composition  
1544 and biogeographic significance. *Estuarine, Coastal and Shelf Science*, 264, 107671

1545 Parent, B., Barras, C., Bicchi, E., Charrieau, L.M., Choquel, C., Bénéteau, É., Maillet, G.M.  
1546 and Jorissen, F.J., 2021. Comparison of four foraminiferal biotic indices assessing the  
1547 environmental quality of coastal Mediterranean soft bottoms. *Water*, 13, 3193

1548 Raposo, D., Frontalini, F., Clemente, I., da Conceição Guerreiro Couto, E., Veríssimo, F. and  
1549 Laut, L., 2022. Benthic foraminiferal response to trace elements in a tropical mesotidal  
1550 Brazilian estuary. *Estuaries and Coasts*, 45, 2610-2631

- 1551 Schmidt, S. and Schönfeld, J., 2021. Living and dead foraminiferal assemblage from the  
 1552 supratidal sand Japsand, North Frisian Wadden Sea: distributional patterns and controlling  
 1553 factors. *Helgoland Marine Research*, 75, 6, 1-22
- 1554 Schumacher, S., Jorissen, F.J., Dissard, D., Larkin, K.E. and Gooday, A.J., 2007. Live (Rose  
 1555 Bengal stained) and dead benthic foraminifera from the oxygen minimum zone of the  
 1556 Pakistan continental margin (Arabian Sea). *Marine Micropaleontology*, 62, 45-73
- 1557 Szarek, R., Kuhnt, W., Kawamura, H. and Kitazato, H., 2006. Distribution of recent benthic  
 1558 foraminifera on the Sunda Shelf (South China Sea). *Marine Micropaleontology*, 61, 171-195
- 1559 Thies, A., 1991. Die Benthos-Foraminiferen im Europäischen Nordmeer. *Doctoral*  
 1560 *dissertation, Christian-Albrechts-Universität Kiel.*
- 1561 Timm, S., 1992. Rezente Tiefsee-Benthosforaminiferen aus Oberflächensedimenten des  
 1562 Golfes von Guinea (Westafrika)-Taxonomie, Verbreitung, Ökologie und  
 1563 Korngrößenfraktionen. *Doctoral dissertation, Geologisch-Paläontologisches Institut und*  
 1564 *Museum Christian-Albrechts-Universität Kiel.*
- 1565 Venturelli, R.A., Rathburn, A.E., Burkett, A.M. and Ziebis, W., 2018. Epifaunal foraminifera  
 1566 in an infaunal World: Insights into the influence of heterogeneity on the benthic ecology of  
 1567 oxygen-poor, deep-sea habitats. *Frontiers in Marine Science*, 5, 344.
- 1568 Walton, W.R., 1955. Ecology of living benthonic foraminifera, Todos Santos Bay, Baja  
 1569 California. *Journal of Paleontology*, 29, 952-1018.
- 1570 Wollenburg, J.E. and Mackensen, A., 1998. Living benthic foraminifers from the central  
 1571 Arctic Ocean: faunal composition, standing stock and diversity. *Marine Micropaleontology*,  
 1572 34, 153-185
- 1573
- 1574 **Supporting references – fossil benthic foraminiferal assemblages**
- 1575 Abu-Zied, R.H., Rohling, E.J., Jorissen, F.J., Fontanier, C., Casford, J.S. and Cooke, S., 2008.  
 1576 Benthic foraminiferal response to changes in bottom-water oxygenation and organic carbon  
 1577 flux in the eastern Mediterranean during LGM to Recent times. *Marine*  
 1578 *Micropaleontology*, 67, 46-68.



1579 Avnaim-Katav, S., Almogi-Labin, A., Schneider-Mor, A., Crouvi, O., Burke, A.A.,  
1580 Kremenetski, K.V. and MacDonald, G.M., 2019. A multi-proxy shallow marine record for  
1581 Mid-to-Late Holocene climate variability, Thera eruptions and cultural change in the Eastern  
1582 Mediterranean. *Quaternary Science Reviews*, 204, 133-148.

1583 Buzas-Stephens, P., Livsey, D.N., Simms, A.R. and Buzas, M.A., 2014. Estuarine  
1584 foraminifera record Holocene stratigraphic changes and Holocene climate changes in ENSO  
1585 and the North American monsoon: Baffin Bay, Texas. *Palaeogeography, Palaeoclimatology,*  
1586 *Palaeoecology*, 404, 44-56.

1587 Cardiff J. et al. 2019. Multidecadal Changes in Marine Subsurface Oxygenation Off Central  
1588 Peru During the Last ca. 170 Years. *Frontiers in Marine Science*, 10.3389/fmars.2019.00270.

1589 Consolaro, C., Rasmussen, T.L. and Panieri, G., 2018. Palaeoceanographic and environmental  
1590 changes in the eastern Fram Strait during the last 14,000 years based on benthic and  
1591 planktonic foraminifera. *Marine Micropaleontology*, 139, 84-101.

1592 Dimiza, M.D., Fatourou, M., Arabas, A., Panagiotopoulos, I., Gogou, A., Kouli, K., Parinos,  
1593 C., Rousakis, G. and Triantaphyllou, M.V., 2020. Deep-sea benthic foraminifera record of the  
1594 last 1500 years in the North Aegean Trough (northeastern Mediterranean): A paleoclimatic  
1595 reconstruction scenario. *Deep Sea Research Part II: Topical Studies in Oceanography*, 171,  
1596 104705.

1597 Filipsson, H.L. and Nordberg, K., 2004. A 200-year environmental record of a low-oxygen  
1598 fjord, Sweden, elucidated by benthic foraminifera, sediment characteristics and hydrographic  
1599 data. *Journal of Foraminiferal Research*, 34, 277-293.

1600 Fink, H.G; Wienberg, C.; Hebbeln, D.; McGregor, H.V.; Schmiedl, G.; Taviani, M.; Freiwald,  
1601 A. (2012): Oxygen control on Holocene cold-water coral development in the eastern  
1602 Mediterranean Sea. *Deep Sea Research Part I: Oceanographic Research Papers*, 62, 89-96

1603 Hess, S., Alve, E., Andersen, T.J. and Joranger, T., 2020. Defining ecological reference  
1604 conditions in naturally stressed environments—How difficult is it? *Marine Environmental*  
1605 *Research*, 156, 104885.

1606 Kaminski, M.A., Aksu, A., Box, M., Hiscott, R.N., Filipescu, S. and Al-Salameen, M., 2002.  
1607 Late Glacial to Holocene benthic foraminifera in the Marmara Sea: implications for Black

1608 Sea–Mediterranean Sea connections following the last deglaciation. *Marine Geology*, 190,  
1609 165-202.

1610 Klootwijk, A.T., Alve, E., Hess, S., Renaud, P.E., S?rlie, C. and Dolven, J.K., 2021.  
1611 Monitoring environmental impacts of fish farms: Comparing reference conditions of sediment  
1612 geochemistry and benthic foraminifera with the present. *Ecological Indicators*, 120, 106818.

1613 Le Houedec, S., Mojtahid, M., Bicchi, E., de Lange, G.J. and Hennekam, R., 2020. Suborbital  
1614 hydrological variability inferred from coupled benthic and planktic foraminiferal?based  
1615 proxies in the southeastern Mediterranean during the last 19 ka. *Paleoceanography and*  
1616 *Paleoclimatology*, 35, e2019PA003827.

1617 Matos, L., Wienberg, C., Titschack, J., Schmiedl, G., Frank, N., Abrantes, F., Cunha, M.R.  
1618 and Hebbeln, D., 2017. Coral mound development at the Campeche cold-water coral  
1619 province, southern Gulf of Mexico: Implications of Antarctic Intermediate Water increased  
1620 influence during interglacials. *Marine Geology*, 392, 53-65.

1621 Melis, R. and Salvi, G., 2009. Late Quaternary foraminiferal assemblages from western Ross  
1622 Sea (Antarctica) in relation to the main glacial and marine lithofacies. *Marine*  
1623 *Micropaleontology*, 70, 39-53.

1624 Melis, R. and Salvi, G., 2020. Foraminifer and Ostracod Occurrence in a Cool-Water  
1625 Carbonate Factory of the Cape Adare (Ross Sea, Antarctica): A Key Lecture for the Climatic  
1626 and Oceanographic Variations in the Last 30,000 Years. *Geosciences*, 10, 413.

1627 Melis, R., Capotondi, L., Torricella, F., Ferretti, P., Geniram, A., Hong, J.K., Kuhn, G., Khim,  
1628 B.K., Kim, S., Malinverno, E. and Yoo, K.C., 2021. Last Glacial Maximum to Holocene  
1629 paleoceanography of the northwestern Ross Sea inferred from sediment core geochemistry  
1630 and micropaleontology at Hallett Ridge. *Journal of Micropalaeontology*, 40, 15-35.

1631 Melis, R., Carbonara, K., Villa, G., Morigi, C., Bárcena, M.A., Giorgetti, G., Caburlotto, A.,  
1632 Rebesco, M. and Lucchi, R.G., 2018. A new multi?proxy investigation of Late Quaternary  
1633 palaeoenvironments along the north-western Barents Sea (Storfjorden Trough Mouth  
1634 Fan). *Journal of Quaternary Science*, 33, 662-676.

1635 Milker, Y., Schmiedl, G. and Betzler, C., 2011. Paleobathymetric history of the Western  
1636 Mediterranean Sea shelf during the latest glacial period and the Holocene: Quantitative

1637 reconstructions based on foraminiferal transfer functions. *Palaeogeography,*  
1638 *Palaeoclimatology, Palaeoecology*, 307, 324-338.

1639 Mojtahid, M., Toucanne, S., Fentimen, R., Barras, C., Le Houedec, S., Soulet, G., Bourillet,  
1640 J.F. and Michel, E., 2017. Changes in northeast Atlantic hydrology during Termination 1:  
1641 Insights from Celtic margin's benthic foraminifera. *Quaternary Science Reviews*, 175, 45-59.

1642 Osterman, L.E. and Smith, C.G., 2012. Over 100 years of environmental change recorded by  
1643 foraminifers and sediments in Mobile Bay, Alabama, Gulf of Mexico, USA. *Estuarine,*  
1644 *Coastal and Shelf Science*, 115, 345-358.

1645 Osterman, L.E., Pavich, K., and Caplan, J., 2004, Benthic foraminiferal census data from Gulf  
1646 of Mexico cores (Texas and Louisiana Continental Shelf). *U.S. Geological Survey Open-File*  
1647 *Report 2001-1209*, 15 p.

1648 Pérez-Asensio, J.N., Frigola, J., Pena, L.D., Sierro, F.J., Reguera, M.I., Rodríguez-Tovar, F.J.,  
1649 Dorador, J., Asioli, A., Kuhlmann, J., Huhn, K. and Cacho, I., 2020. Changes in western  
1650 Mediterranean thermohaline circulation in association with a deglacial Organic Rich Layer  
1651 formation in the Alboran Sea. *Quaternary Science Reviews*, 228, 106075.

1652 Pinto, A.F.S., Martins, M.V.A., Fonseca, M.C.M., Pereira, E., Terroso, D.L., Rocha, F.,  
1653 Rodrigues, M.A.C., 2017. Late Holocene closure of a barrier beach in Sepetiba Bay and its  
1654 environmental impact (Rio de Janeiro, Brazil). *Journal of Sedimentary Environments*, 2, 65-  
1655 80.

1656 Polovodova Asteman, I. and Nordberg, K., 2013. Foraminiferal fauna from a deep basin in  
1657 Gullmar Fjord: The influence of seasonal hypoxia and North Atlantic Oscillation. *Journal of*  
1658 *Sea Research*, 79, 40-49.

1659 Polyak, L., Best, K.M., Crawford, K.A., Council, E.A. and St-Onge, G., 2013. Quaternary  
1660 history of sea ice in the western Arctic Ocean based on foraminifera. *Quaternary Science*  
1661 *Reviews*, 79, 145-156.

1662 Richwine, K.A., Marot, M., Smith, C.G., Osterman, L.E. and Adams, C.S., 2013. Biological  
1663 and geochemical data of gravity cores from mobile Bay, Alabama. *US Department of the*  
1664 *Interior, US Geological Survey*.

- 1665 Schmiedl, G., Hemleben, C., Keller, J. and Segl, M., 1998. Impact of climatic changes on the  
1666 benthic foraminiferal fauna in the Ionian Sea during the last 330, 0000  
1667 years. *Paleoceanography*, 13, 447-458.
- 1668 Schmiedl, G., Mitschele, A., Beck, S., Emeis, K.C., Hemleben, C., Schulz, H., Sperling, M.  
1669 and Weldeab, S., 2003. Benthic foraminiferal record of ecosystem variability in the eastern  
1670 Mediterranean Sea during times of sapropel S5 and S6 deposition. *Palaeogeography*,  
1671 *Palaeoclimatology, Palaeoecology*, 190, 139-164.
- 1672 Takata, H., Hong, S.H., Yoo, D.G., Kim, J.C., Cheong, D. and Khim, B.K., 2022. Fossil  
1673 benthic foraminifera in the Nakdong River Delta (southeast Korea) during the early to middle  
1674 Holocene. *Paleontological Research*, 26, 283-300.
- 1675 Tetard, M., Licari, L. and Beaufort, L., 2017. Oxygen history off Baja California over the last  
1676 80 kyr: A new foraminiferal?based record. *Paleoceanography*, 32, 246-264.
- 1677 Tsujimoto, A., Nomura, R., Yasuhara, M., Yamazaki, H. and Yoshikawa, S., 2006. Impact of  
1678 eutrophication on shallow marine benthic foraminifers over the last 150 years in Osaka Bay,  
1679 Japan. *Marine Micropaleontology*, 60, 258-268.
- 1680 Usami, K., Ohi, T., Hasegawa, S. and Ikehara, K., 2013. Foraminiferal records of bottom-  
1681 water oxygenation and surface-water productivity in the southern Japan Sea during 160–15  
1682 ka: associations with insolation changes. *Marine Micropaleontology*, 101, 10-27.
- 1683 Xiang, R., Yang, Z., Saito, Y., Fan, D., Chen, M., Guo, Z. and Chen, Z., 2008.  
1684 Paleoenvironmental changes during the last 8400 years in the southern Yellow Sea: Benthic  
1685 foraminiferal and stable isotopic evidence. *Marine Micropaleontology*, 67, 104-119.